Tamaki K, Sasano H, Maruo Y, Takahashi Y, Miyashita M, Moriya T, Sato Y, Hirakawa H, Tamaki N, Watanabe M, Ishida T, Ohuchi N (2010) Vasohibin-1 as a potential predictor of aggressive behavior of ductal carcinoma *in situ* of the breast. *Cancer Sci* **101**: 1051–1058.

Watanabe K, Hasegawa Y, Yamashita H, Shimizu K, Ding Y, Abe M, Ohta H, Imagawa K, Hojo K, Maki H, Sonoda H, Sato Y (2004) Vasohibin as an endothelium-derived negative feedback regulator of angiogenesis. *J Clin Invest* **114**: 898–907.

Weidner N, Semple JP, Welch WR, Folkman J (1991) Tumor angiogenesis and metastasis – correlation in invasive breast carcinoma. *N Engl J Med* **324**: 1–8.

Weidner N, Carroll PR, Flax J, Blumenfeld W, Folkman J (1993) Tumor angiogenesis correlates with metastasis in invasive prostate carcinoma. *Am J Pathol* **143**: 401–409.

Yoshinaga K, Ito K, Moriya T, Nagase S, Takano T, Niikura H, Sasano H, Yaegashi N, Sato Y (2011) Roles of intrinsic angiogenesis inhibitor, vasohibin, in cervical carcinomas. *Cancer Sci* **102**: 446–451.

Yoshinaga K, Ito K, Moriya T, Nagase S, Takano T, Niikura H, Yaegashi N, Sato Y (2008) Expression of vasohibin as a novel endothelium-derived angiogenesis inhibitor in endometrial cancer *Cancer Sci* **99**: 914–919.

HYBRIDOMA
Volume 31, Number 4, 2012

DOI: 10.1089/hyb.2012.0021

Monoclonal Antibody Selectively Recognizing Murine But Not Human CD44

Yumi Kinugasa[1] and Nobuyuki Takakura[1,2]

Here we report on the generation of a monoclonal antibody (MAb) specific for murine, but not human CD44 obtained by immunization with cancer-associated fibroblasts. The monoclonal antibody MS44 recognizes CD44, as evidenced by immunoblotting of cell lysates. Additionally, MAb MS44 reacts with mouse but not human CD44 in flow cytometry. Thus, this antibody provides an effective tool to analyze CD44 from host (mouse) cells in human cancer cell xenograft models in mice.

Introduction

THE TUMOR ENVIRONMENT CONSISTS of stromal cell components, including endothelial cells, activated fibroblasts, inflammatory cells, and others, together with the extracellular matrix. In the tumor stroma, cancer-associated fibroblasts (CAFs) are a major component, contributing to tumor initiation, growth, and progression. Recent studies show that there are several different subpopulations of CAFs expressing partially overlapping markers, including α-smooth muscle actin, platelet-derived growth factor (PDGF) receptors, fibroblast specific protein-1, and others.[1,2]

CD44 is a class I transmembrane glycoprotein expressed ubiquitously in a number of isoforms generated by alternative splicing of 10 exons.[3] It has been reported that some variant isoforms of CD44 (CD44v) induced a metastatic phenotype.[4] Therefore, CD44v is implicated as a cancer-initiating cell marker in several cancers.[5,6] In contrast, the shortest, standard or hematopoietic, isoform (CD44s) is expressed on the membrane of most vertebrate cells.[3] CD44s is an adhesion molecule that is upregulated following tissue injury and is implicated in many chronic inflammatory diseases such as rheumatoid arthritis.[7–10]

Here we report the production of a monoclonal antibody (MAb) raised against cloned tumor stromal cells, CAFs, and show by immunoblotting and flow cytometry that it specifically recognizes murine, but not human CD44s.

Materials and Methods

Cell culture and animals

Mouse melanoma cell line (B16) and African green monkey kidney fibroblast-like cell line (COS7) were maintained in DMEM (Sigma, St. Louis, MO) with 10% fetal bovine serum (FBS, Sigma) and penicillin/streptomycin (Invitrogen, Carlsbad, CA). Human umbilical vein endothelial cells (HUVEC) were maintained in Humedia EG2 (Kurabo, Osaka, Japan). The animals were housed in environmentally controlled rooms of the animal experimentation facility at Osaka University. All experiments were done in compliance with the laws and institutional guidelines of Osaka University.

Immunohistochemical staining

Tissue fixation, preparation of tissue sections, and staining of sections with antibodies were performed as described previously.[11] For immunohistochemistry, rat anti-PDGFRβ antibody (APB5, eBioscience, San Diego, CA) and phycoerythrin (PE)-conjugated anti-rat IgG antibody (BD Biosciences, San Jose, CA) were used. Stained sections were assessed using a CTR 5500 (Leica, Wetzlar, Germany).

Establishment of tumor stromal cell lines

Tumor stromal cells defined as CAFs were isolated from B16 melanoma xenografts in CAG-EGFP/C57BL/6 mice (Jackson ImmunoResearch Laboratory, West Grove, PA). Single cell suspensions of tumor tissues were prepared using a standard protocol. The antibodies used for flow cytometry were biotin-conjugated APB5 (eBioscience), PE-conjugated anti-lineage (a mixture of ter119, Gr-1, Mac-1, B220, CD4, and CD8), and CD31 antibodies (all purchased from BD Biosciences). Biotinylated antibodies were visualized with APC-conjugated streptavidin (BD Biosciences). Cell sorting was done by JSAN (Bay Bioscience, Kobe, Japan). GFP^+ Lin^- $CD31^-$ $PDGFR\beta^+$ cells were isolated as CAFs and grown in DMEM with 10% FBS and penicillin/streptomycin. CAFs were immortalized with the simian virus 40 large T antigen (SV40LT, a gift of Dr. M. Yutsudo) and cloned.

[1]Department of Signal Transduction, Research Institute for Microbial Diseases, Osaka University, Suita, Osaka, Japan.
[2]JST, CREST, K's Gobancho, Chiyoda-ku, Tokyo, Japan.

Preparation of cell extracts for use as antigen

The collected cells were washed with ice-cold phosphate-buffered saline (PBS) and lysed in an ice-cold lysis buffer I (1 mM EDTA, 50 mM Tris-HCl [pH 7.6], 150 mM NaCl, supplemented with Complete Protease Inhibitor Cocktail [Roche, Indianapolis, IN]). The cell lysates were homogenized using a PT 3100 polytron homogenizer (Ishii Laboratory Works, Osaka, Japan) and centrifuged at 20,400 *g* for 15 min. Pellets were suspended in ice-cold lysis buffer II (1% NP-40, 1 mM EDTA, 50 mM Tris-HCl [pH 7.6], 150 mM NaCl, Complete Protease Inhibitor Cocktail), sonicated, and centrifuged at 20,400 *g* for 10 min. The supernatants were collected as cell extracts.

Production of monoclonal antibody

CAF cell extracts were used as antigen to immunize rats, and rat/mouse hybridomas were established by standard procedures.[12] The mouse myeloma cell line X63Ag8653 was used for cell fusion. A stable hybridoma cell line, MS44, was obtained.

ELISA

The cell extracts in 1% bovine serum albumin (Sigma) in PBS (1% BSA/PBS) were absorbed to the surface of 96-well plates (Becton Dickinson, Franklin Lakes, NJ) overnight at 4°C. To avoid non-specific binding, the plates were blocked with 5% BSA/PBS. The hybridoma supernatants were incubated for 2 h at room temperature, then washed three times with 0.05% Tween-20 in PBS (T-PBS). The plates were incubated for 1 h at room temperature with horseradish peroxidase (HRP)-conjugated anti-rat IgG antibody (BioSource, Camarillo, CA). After washing with T-PBS five times, immunoreactivity was visualized with substrate 3,3′,5,5′-Tetramethylbenzidine (Wako Pure Chemical Industries, Osaka, Japan) and absorbance measured by Powerscan HT (DS Pharma Biomedical, Osaka, Japan).

Immunoprecipitation and immunoblotting

CAF cell extracts were incubated with MAb MS44 or rat IgG2b, κ isotype control (eBioscience) for 2 h at 4°C with end-over-end rotation. Protein G-Sepharose beads (GE Healthcare, Buckinghamshire, United Kingdom) were added to lysate/antibody mixture and incubated for 2 h at 4°C. The mixture was centrifuged and the Protein G-Sepharose beads were washed three times with lysis buffer. Bound proteins were analyzed by immunoblotting using MAb MS44 as the primary antibody. HRP-conjugated anti-rat IgG antibody (Invitrogen) was used as the secondary antibody. The immunoreactive proteins were visualized using the ECL plus Western Blotting Detection system (GE Healthcare). The blots were scanned with a imaging densitometer (LAS-3000 Mini, Fujifilm, Tokyo, Japan).

Identification of antigen recognized by MAb MS44 using LC-MS/MS

The purified protein complexes were separated by SDS-PAGE on a 5–20% gradient gel (DRC, Tokyo, Japan). After visualization of the proteins by silver staining (Daiichi Pure Chemicals, Tokyo, Jpaan), the specific band was excised from the gel and digested *in situ* with TrypsinGold (Promega, Madison, WI). The digested samples were analyzed using a QTOF Ultima (Waters, Milford, MA), as described previously.[13]

Expression vector and transient expression

For transient expression in COS7 cells, the full-length mouse CD44s and full-length human CD44s were cloned into the BglII and XhoI sites of modified pME18S vector (pME18S-V5).[14] Transfection was carried out using Lipofectamine 2000 (Invitrogen). COS7 cell extracts, or extracts of cells expressing V5-tagged mouse CD44s (mCD44-V5) or V5-tagged human CD44s (hCD44-V5), were analyzed by immunoblotting with MAb MS44, anti-V5 mouse monoclonal antibody (Invitrogen), and anti-mouse/human CD44 rat monoclonal antibody (IM7, eBioscience) by the methods described above.

FACS analysis

FACS analysis was performed as described previously[11] using DyLight 649 (Thermo, Rockford, IL)-conjugated MAb MS44 and APC-conjugated IM7 (eBioscience).

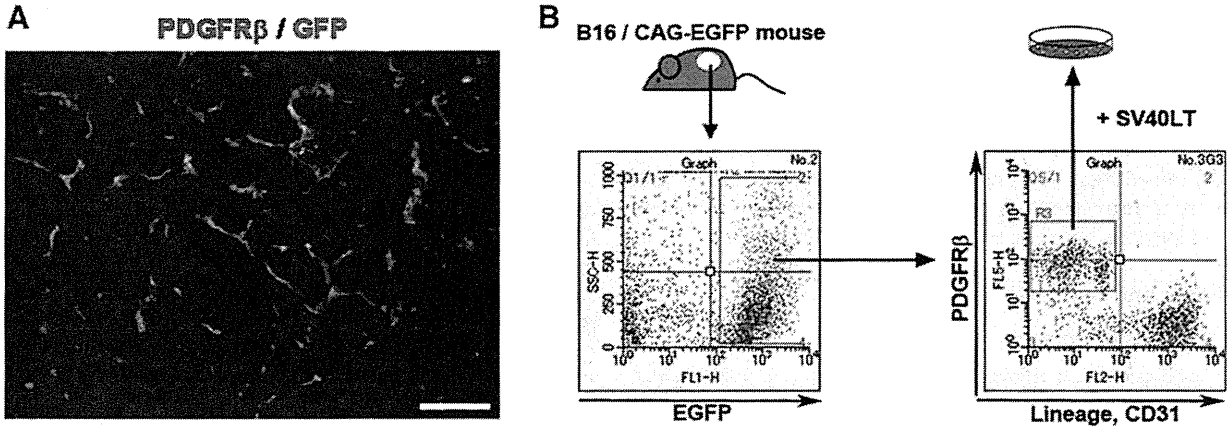

FIG. 1. Expansion of cancer-associated fibroblasts. (**A**) Expression of PDGFRβ (red) and endogenous GFP (green) in tumor tissue generated by inoculation of B16 melanoma cells into a CAG-EGFP mouse. Bar indicates 100 μm. (**B**) Schematic of strategy for establishment of CAF cell lines isolated from B16 melanoma-bearing CAG-EGFP mice. CAFs (right) defined as Lin^- $CD31^-$ $PDGFR\beta^+$ cells were isolated from GFP^+ host mouse-derived cells (left), immortalized with the simian virus 40 large T antigen (SV40LT), and cloned and expanded for the preparation of cell lysate.

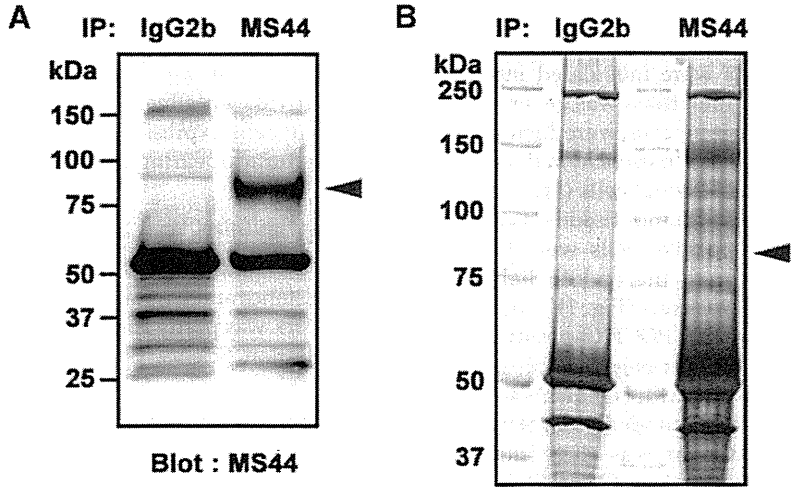

FIG. 2. Identification of MAb MS44 antigen. Cell lysates were prepared from cloned CAFs and immunoprecipitated with MAb MS44. The samples pulled down were immunobloted with MAb MS44 (A) stained with silver (B). IgG2b was the isotype-matched control Ig. The specific band (arrowhead) was analyzed by LC-MS/MS.

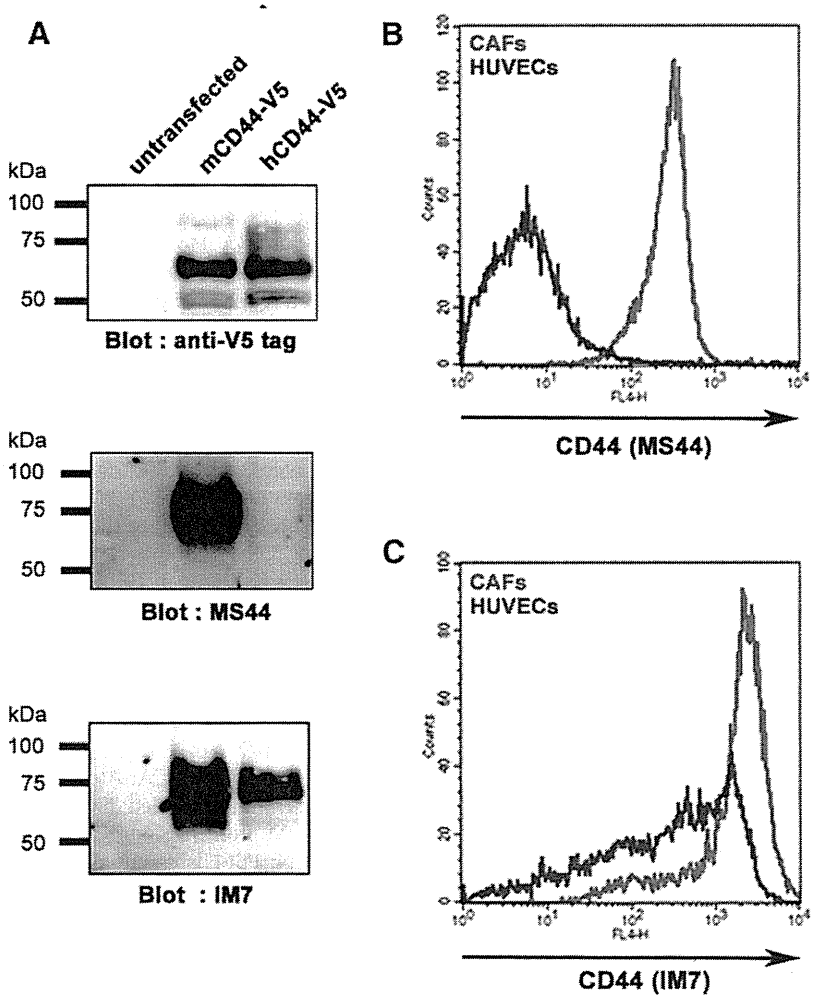

FIG. 3. Specificity of MAb MS44 for mouse CD44. (A) Extracts of COS7 cells transiently expressing V5-tagged mouse CD44s (mCD44-V5) or human CD44s (hCD44-V5) were analyzed by Western blot analysis using anti-V5 antibody (upper panel), MAb MS44 (middle panel), and anti-mouse/human CD44 antibody IM7 (lower panel). CAFs (red) or HUVECs (blue) were stained with MAb MS44 (B) or IM7 (C) and analyzed by flow cytometry.

Results and Discussion

B16 mouse melanoma cells were inoculated into CAG-EGFP/C57BL/6 mice and a tumor mass was generated. The host mouse-derived GFP-positive cells were histologically of two types: PDGFRβ-positive mesenchymal cells and PDGFRβ−negative non-mesenchymal cells (Fig. 1A). Analysis of single cell suspensions of tumor tissue revealed that approximately 50% of GFP-positive cells were PDGFRβ-positive and did not co-express the endothelial marker CD31 or other hematopoietic markers (Fig. 1B). To identify CAF-specific molecules, we sorted PDGFRβ-positive, CD31-negative, or hematopoietic marker-negative cells. To establish immortalized CAFs, we transduced the SV40LT gene into sorted cells and cloned and expanded them. An 8-week-old female F344/N Slc (SLC) rat was then immunized with cell extracts of these immortalized CAFs. Hybridomas obtained after fusing B lymphocytes from spleen of the immunized rat with mouse myeloma cells were tested by ELISA for the production of MAbs that reacted with the CAF cell extracts. Twenty-three supernatants, positive by ELISA, were further examined by immunoprecipitation and Western blot analysis to determine whether the MAb recognized multiple non-specific proteins (data not shown). One of these MAbs, designated MS44, was selected for further study.

To identify the antigen recognized by MAb MS44, CAF cell extracts were immunoprecipitated and the bound proteins separated on an SDS-PAGE gel (Fig. 2). LC-MS/MS analysis of the visible bands (Fig. 2B) resulted in the identification of CD44.

We transduced mouse (m) and human (h) CD44 fused with a V5 tag epitope into COS7 cells and tested for cross-reactivity of MS44 on human CD44. We confirmed a similar level of mCD44 and hCD44 expression in transfected COS7 cells by detection of V5 (Fig. 3A). IM7, a commercially available anti-CD44 (IM7) MAb, recognized both mCD44 and hCD44; however, our MS44 recognized mCD44 but not hCD44 (Fig. 3A). MS44 no longer recognized CD44 deglycosylated by N-Glycanase treatment (data not shown). Therefore, we conclude that MS44 recognizes sugar moieties of the extracellular domain of CD44.

Next we applied flow cytometry to analyze human umbilical vein endothelial cells (HUVECs), which express CD44[15] and CAFs. We found that MAb MS44 stained mouse CD44 on CAFs, but not human CD44 on HUVECs (Fig. 3B). On the other hand, IM7 recognized both mCD44 and hCD44 on these cells (Fig. 3C). These results suggest that MAb MS44 is specific for murine but not human CD44.

As reported here, CD44 is expressed abundantly in CAFs and is probably involved in the formation of the tumor microenvironment. Functional analysis of CD44 in non-cancer cells may shed light on the development of new strategies for managing cancer patients. To this end, it is important to analyze the localization of CD44-positive CAFs in tumor tissue precisely. Because cancer cells may also express CD44, this may perturb visualization of CD44-positive CAFs in the tumor microenvironment when a syngeneic mouse cancer model or chemically and/or genetically induced cancer models in mice are used. However, in a model where human cancer cells are inoculated into nude mice, MS44 will detect host mouse-derived CAFs but not human cancer cells. We have confirmed that MS44 is suitable for use in immunohistochemistry. Therefore the monoclonal anti-mouse CD44-specific antibody MAb MS44 will provide an effective tool for investigating the localization of cells expressing CD44 in tumor stromal tissues of human tumor-bearing mice.

Acknowledgments

We thank Ms. Keisho Fukuhara and Ms. Noriko Fujimoto for assistance and Dr. Kazunobu Saito for technical assistance. This work was partly supported by a grant from the Ministry of Education, Science, Sports, and Culture of Japan.

Author Disclosure Statement

The authors have no financial interests to disclose.

References

1. Sugimoto H, Mundel TM, Kieran MW, and Kalluri R: Identification of fibroblast heterogeneity in the tumor microenvironment. Cancer Biol Ther 2006;5:1640–1646.
2. Anderberg C, Li H, Fredriksson L, Andrae J, Betsholtz C, Li X, Eriksson U, and Pietras K: Paracrine signaling by platelet-derived growth factor-CC promotes tumor growth by recruitment of cancer-associated fibroblasts. Cancer Res 2009; 69:369–378.
3. Screaton GR, Bell MV, Jackson DG, Cornelis FB, Gerth U, and Bell JI: Genomic structure of DNA encoding the lymphocyte homing receptor CD44 reveals at least 12 alternatively spliced exons. Proc Natl Acad Sci USA 1992;89: 12160–12164.
4. Günthert U, Hofmann M, Rudy W, Reber S, Zöller M, Haussmann I, Matzku S, Wenzel A, Ponta H, and Herrlich P: A new variant of glycoprotein CD44 confers metastatic potential to rat carcinoma cells. Cell 1991;65:13–24.
5. Naor D, Wallach-Dayan SB, Zahalka MA and Sionov RV: Involvement of CD44, a molecule with a thousand faces, in cancer dissemination. Semin Cancer Biol 2008;18:260–267.
6. Ratajczak MZ: Cancer stem cells—normal stem cells "Jedi" that went over to the "dark side." Folia Histochem Cytobiol 2005;43:175–181.
7. Holgate ST: Asthma: a dynamic disease of inflammation and repair. Ciba Found Symp 1997;206:106–110.
8. Mikecz K, Brennan FR, Kim JH, and Glant TT: Anti-CD44 treatment abrogates tissue oedema and leukocyte infiltration in murine arthritis. Nat Med 1995;1:558–563.
9. Jain M, He Q, Lee WS, Kashiki S, Foster LC, Tsai JC, Lee ME, and Haber E: Role of CD44 in the reaction of vascular smooth muscle cells to arterial wall injury. J Clin Invest 1996;98:877.
10. Puré E, and Cuff CA: A crucial role for CD44 in inflammation. Trends Mol Med 2001;7:213–221.
11. Ueno M, Itoh M, Kong L, Sugihara K, Asano M, and Takakura N: PSF1 is essential for early embryogenesis in mice. Mol Cell Biol 2005;25:10528–10532.
12. Takakura N, Yoshida H, Ogura Y, Kataoka H, Nishikawa S, and Nishikawa S: PDGFR alpha expression during mouse embryogenesis: immunolocalization analyzed by whole-mount immunohistostaining using the monoclonal anti-mouse PDGFR alpha antibody APA5. J Histochem Cytochem 1997;45:883–893.
13. Saito K, Enya K, Oneyama C, Hikita T, and Okada M: Proteomic identification of ZO-1/2 as a novel scaffold for

Src/Csk regulatory circuit. Biochem Biophys Res Commun 2008;366:969–975.
14. Hieda M, Isokane M, Koizumi M, Higashi C, Tachibana T, Shudou M, Taguchi T, Hieda Y, and Higashiyama S: Membrane-anchored growth factor, HB-EGF, on the cell surface targeted to the inner nuclear membrane. J Cell Biol 2008;180:763–769.
15. Taniguchi K, Harada N, Ohizumi I, Tsutsumi Y, Nakagawa S, Kaiho S, and Mayumi T: Recognition of human activated CD44 by tumor vasculature-targeted antibody. Biochem Biophys Res Commun 2000;269:671–675.

Address correspondence to:
Prof. Nobuyuki Takakura
Department of Signal Transduction
Research Institute for Microbial Diseases
Osaka University
3-1 Yamada-oka
Suita
Osaka 565-0871
Japan

E-mail: ntakaku@biken.osaka-u.ac.jp

Received: March 8, 2012
Accepted: May 1, 2012

J. Biochem. 2012;152(2):125–131 doi:10.1093/jb/mvs071

JB THE JOURNAL OF BIOCHEMISTRY

JB Review

Biology of the apelin-APJ axis in vascular formation

Received May 14, 2012; accepted June 12, 2012; published online June 28, 2012

Hiroyasu Kidoya[1,*] and Nobuyuki Takakura[1,2,†]

[1]Department of Signal Transduction, Research Institute for Microbial Diseases, Osaka University, 3-1 Yamada-oka, Suita, Osaka 565-0871, Japan; and [2]Japan Science and Technology Agency, Core Research for Evolution Science and Technology, K's Gobancho, 7 Gobancho, Chiyoda-ku, Tokyo 102-0076, Japan

*Hiroyasu Kidoya, Department of Signal Transduction, Research Institute for Microbial Diseases, Osaka University, 3-1 Yamada-oka, Suita, Osaka 565-0871, Japan. Tel: +81-66-879-8312, Fax: +81-66-879-8314, email: kidoya@biken.osaka-u.ac.jp

†Present address: Nobuyuki Takakura, Department of Signal Transduction, Research Institute for Microbial Diseases, Osaka University, 3-1 Yamada-oka, Suita, Osaka 565-0871, Japan.

Apelin is a bioactive peptide with diverse physiological actions on many tissues mediated by its interaction with its specific receptor APJ. Since the identification of apelin and APJ in 1998, pleiotropic roles of the apelin/APJ system have been elucidated in different tissues and organs, including modulation of the cardiovascular system, fluid homeostasis, metabolic pathway and vascular formation. In blood vessels, apelin and APJ expression are spatiotemporally regulated in endothelial cells (ECs) during angiogenesis. *In vitro* analysis revealed that the apelin/APJ system regulates angiogenesis by the induction of proliferation, migration and cord formation of cultured ECs. Moreover, apelin seems to stabilize cell–cell junctions of ECs. In addition, genetically engineered mouse models suggest that apelin/APJ regulates vascular stabilization and maturation in physiological and pathological angiogenesis. In this review, we summarize the current understanding of the apelin/APJ system for vascular formation and maturation.

Keywords: apelin and APJ/development/regenerative medicine/tumour angiogenesis/vascular formation.

Abbreviations: bFGF, basic fibroblast growth factor; CAM, chorioallantoic membrane; DCs, dendritic cells; ECs, endothelial cells; ERK, extracellular-regulated kinases; HIF, hypoxia inducible factor; iNKT, invariant natural killer T; ISVs, intersomitic vessels; PI3K, phosphatidylinositol-3 kinase; VEGF, vascular endothelial growth factor.

Characteristics of Apelin and APJ

Apelin was initially identified as an endogenous ligand for the orphan G protein-coupled receptor with seven transmembrane domains, APJ, isolated from bovine stomach extracts in 1998 (*1*). Apelin is secreted as a 77 amino acid pre-proprotein, an immature peptide, which is cleaved by protease to form C-terminal products, including apelin-13, apelin-17 and apelin-36 (*2*). These isoforms have distinct activities, with the shorter isoform seeming to be the more potent activator for APJ. In mammals, the sequence of preproapelin is strongly conserved in different species, and it has complete identity for the last 23 residues of the C-terminal. Apelin (65–77) activates extracellular signal-regulated kinases through a pertussis toxin sensitive G protein (*3*). Apelin-13 and apelin-36 have different receptor binding affinity and cause different intracellular trafficking of APJ (*4*). The gene encoding the APJ receptor was identified by homology cloning in 1993 (*5*). APJ has high-sequence homology with the angiotensin II type I receptor, but it does not bind angiotensin II. Apelin is believed to be the only endogenous ligand for APJ.

Apelin and APJ mediate a wide range of physiological actions, including regulation of cardiovascular function, fluid homeostasis, adipo-insular axis and angiogenesis. Studies on APJ function have been focused on the cardiovascular system, because of its similarity to the angiotensin II receptor. It seems that intravenous injection of apelin induces a reduction in blood pressure (*6*). The hypotensive effect of apelin is a consequence of intracellular activation of nitric oxide synthase (*7*). Apelin also causes vasoconstriction because of contraction of the vascular smooth muscle cells (*8*). Plasma apelin levels and APJ expression are clearly modulated in patients with heart failure (*9*, *10*). It has been reported that apelin has positive inotropic effects in *in vitro* and *in vivo* studies (*11–14*). Apelin has been shown to be expressed and released from adipocytes by fasting and refeeding factors, such as insulin, and can act as an adipokine (*15*). For these reasons, apelin is now attracting attention in the context of metabolic disease. In patients with type 2 diabetes, plasma apelin concentrations are increased (*16*, *17*). It has also been suggested that apelin may have other effects, such as on fluid homeostasis (*18*), gastrin stimulation (*19*) and immune responses (*20*).

Distribution and Regulation of Expression of Apelin and APJ

Tissue and cellular distribution

In mammals, APJ expression is widely distributed in various peripheral tissues of adult and embryo. Highest levels of APJ are found in the lung and heart, and significant but lower levels of APJ mRNA are present in skeletal muscle, pituitary gland, kidney and ovary (*21*) (*22*). In these tissues, APJ expression was localized in the vascular and endocardial

endothelial cells (ECs) and smooth muscle cells (*23*). APJ expression is also observed in the brain, including the cerebral cortex, hypothalamus, hippocampus and pituitary gland (*6*, *22*). Apelin expression is also detected in a range of peripheral tissues, including heart, liver, kidney, adipose tissues and brain, with highest levels found in the lung and the mammary gland (*2*, *6*, *20*, *24*). Localization of apelin expression in tissue was observed in vascular ECs, adipose tissue and epithelial cells (*7*).

An important physiological role for apelin and APJ is suggested by the observation of widespread distribution of receptor and ligand expression in tissues, as described previously. Apelin and APJ were found to be abundantly expressed in various peripheral tissues, and localization was restricted to blood vessels (*2*, *7*, *8*, *20*, *22–26*), suggesting a role for apelin/APJ in angiogenesis and vascular formation.

Regulation of transcription

Many transcription factors that may regulate apelin gene expression have been reported. Rat and human apelin core promoter sequences contain putative binding sites for upstream stimulatory factor 1/2, and overexpression of USF upregulates apelin transcription (*27*). Multiple signal transducer and activator of transcription binding sites have been identified in the rat apelin promoter, and apelin expression is elicited by stimulation using inflammatory cytokines associated with binding of phospho-Stat3 (*28*). In white adipocytes, apelin is upregulated by the transcriptional co-activator peroxisome proliferator-activated receptor γ co-activator 1 α (*29*). Under hypoxic conditions, hypoxia inducible factor-1α (HIF1-α) binds to the hypoxia-responsive element (-813/-826) located within the first intron of the human apelin gene and increases apelin expression in vascular cells (*30*).

The molecular mechanism of APJ gene transcriptional regulation has not been well characterized so far. Analysis of the 5′-flanking region of a rat APJ genomic clone identified sites with the strongest promoter activity in a region between (-966/-165) where the Sp1 motif suggested to play a major role (*31*). Other investigations using gene-based single-nucleotide polymorphism analysis have also shown that both APJ and apelin genes are probably regulated by Sp1 (*32*).

Cell effects and intracellular responses

Apelin has been shown to induce the proliferation and migration of APJ-expressing ECs (*33*). The major signalling pathways of apelin are mediated initially by Gi-protein coupled to the APJ receptor and protein kinase C (Fig. 1). It has been reported that apelin causes concentration-dependent inhibition of forskolin-stimulated production of cAMP and increases the phosphorylation of extracellular-regulated kinases (ERK) or protein kinase B in umbilical ECs (*3*, *20*). Apelin/APJ-induced ERK activation is mediated by pertussis toxin sensitive G protein (*3*). On binding of apelin to APJ, the phosphatidylinositol-3 kinase (PI3K) pathway and the ERK pathway lead to the phosphorylation of p70S6K. It has been reported that the PI3K-protein kinase B pathway contributes to EC migration (*34*) and that the ERK/PI3K-p70S6K pathway regulates EC proliferation (*35*). Acceleration of cell motility by apelin was also reported using Chinese hamster ovary cells expressing APJ (*21*). Recently, it has been shown that APJ forms a heterodimer with κ-opioid receptors and leads to phosphorylation of ERK, resulting in increased cell proliferation (*36*). In addition, apelin inhibits the mouse pulmonary arterial EC apoptosis, observed in pulmonary arterial hypertension (*37*). It has been reported that apelin-induced anti-apoptosis is mediated by the induction of Bcl2 protein expression and activation of the PI3K/protein kinase B signalling pathway (*38*). Apelin-36 and apelin-13 can activate the same set of intracellular effectors, but they display some differences in their Gi-protein coupling and differ greatly in their desensitization pattern (*39*).

Role of Apelin in Blood Vessel Formation

Developmental stage

The establishment of vascular network is absolutely necessary for the growth and maintenance of tissues/organs. New blood vessel formation in vertebrates is known to occur by two different processes, vasculogenesis and angiogenesis (*40*). Vasculogenesis is the process of formation of *de novo* primitive vascular networks directly from angioblastic precursor cells. In contrast, angiogenesis is a process of formation of new vascular segments by sprouting from the pre-existing vessels. Vasculogenesis is normally observed in early embryogenesis, whereas angiogenesis occurs during development and in post-natal life.

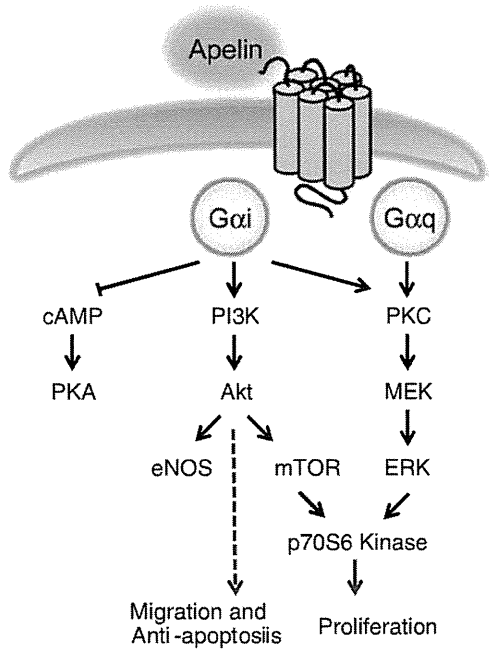

Fig. 1 Schematic of intracellular signal transduction pathways and cellular effects in the apelin/APJ system.

Apelin seems to have important roles in angiogenesis during embryogenesis. In *Xenopus laevis* embryos, expression of homologues of apelin and APJ are observed in developing vascular structures of the inter-somitic vein (*41*). Implantation of beads carrying apelin peptide stimulated prominent outgrowth of ECs and, conversely, morpholino-based translational inhibition of apelin and APJ suppressed inter-segmental angiogenesis (*42*). During segmentation of zebrafish embryos, expression of an ortholog of APJ is observed in epithelial structures, such as venous vasculature (*43*). Consistent with these results, APJ is expressed on ECs in newly formed blood vessels in mouse embryos. At E8.5, APJ expression was observed in ECs that had sprouted from the dorsal aorta, but not in those that were forming the dorsal aorta by the process of vasculogenesis. At E9.5, APJ expression was observed in the migrating end region of inter-somitic vessels sprouting from the dorsal aorta, gradually disappearing as the blood vessels matured. Furthermore, apelin protein was also detected in the somite region at E9.5 (*44*). These expression profiles suggest that the apelin/APJ system plays a spatiotemporal role in blood vessel formation by its transient expression on blood vessels ECs during angiogenesis. The role of apelin in vascular formation has been studied in our group using mouse embryos. We previously showed that the apelin/APJ system induces cell–cell assembly and the proliferation of vascular ECs. When the apelin gene was knocked out, the caliber of inter-somatic vessels in the embryo was narrower. These results indicated that the apelin/APJ system is involved in maturation of blood vessels by caliber size modification during angiogenesis (*44*) (Fig. 2).

In the neonatal mouse retina, APJ expression is upregulated in ECs of the radial vessels sprouting from the optic nerve head region, but attenuated after vessel stabilization. Expression of the apelin gene was also observed in the sprouts of extending vessels at the leading edge (*45*, *46*). During sprouting angiogenesis, growing vascular capillaries are spearheaded by specialized ECs, termed outgrowing tip cells, which act as a guide for the direction of migration of newly developed blood vessels. Behind the tip cells, proliferating ECs, termed stalk cells, induce elongation of the blood vessels, and tip and stalk cells are dynamically challenged and replaced alternately during sprouting angiogenesis (*47*, *48*). Recently, apelin was identified as one of the genes with high expression in tip cells and has been suggested to modulate proliferation of stalk cells expressing the APJ receptor (*49*) (Fig. 2); therefore, apelin-APJ signalling may have a role in tip-cells and stalk-cells characterization. Using apelin-deficient mice, it was suggested that the apelin/APJ system participates in retinal vascularization and ocular development by modulating the angiogenic response to vascular endothelial growth factor (VEGF) and/or basic fibroblast growth factor (*50*). Moreover, we recently proposed that apelin/APJ activation in ECs is a trigger for finalization of blood vessel formation, indirectly mediated by the induction of astrocyte maturation (*51*). During development of the retinal vasculature, APJ mRNA expression is specifically restricted to the venules and the associated capillaries (*46*), indicating a possible function of apelin signalling for venous vascular formation.

Tumour angiogenesis

Apelin has been reported to be broadly expressed in ECs of tumours of different origins. By comparing gene expression profiles in tumours versus normal endothelium, apelin has been identified as a tumour endothelial-specific gene (*52*). In human breast carcinoma, apelin expression was detected in the vascular ECs by immunohistochemical analysis (*53*). As described previously, apelin expression is physiologically modulated by tissue hypoxia and regulated by HIF-1α (*30*). The hypoxic tumour microenvironment may thus induce HIF1α-dependent apelin expression in tumour ECs.

It has been reported that the expression level of the APJ receptor is also increased in tumour endothelium. In glioblastoma, both APJ and apelin transcripts are highly upregulated within the microvasculature compared with blood vessels in normal brain tissue (*41*). Consistent with this result, we detected high-level expression of apelin and APJ mRNA in ECs from tumours generated by the inoculation of Lewis lung carcinoma and colon 26 adenocarcinoma cells into mice. In addition, immunohistochemical analysis of colon 26 tumour revealed that ~13% and 27% of the vessels were APJ-positive and apelin-positive, respectively, and most ECs co-expressed apelin and APJ (*54*). Of course, the ratios of apelin or APJ positivity in ECs may be different depending on the tumour size and tumour growth course. Observation of high APJ expression in angiogenic blood vessels in tumours was similar to that during normal development. Co-expression of ligand and receptor in ECs of the newly formed tumour blood vessels suggests the possibility that APJ in ECs is stimulated by autocrine and paracrine loops.

Several attempts have been made to determine the role of the apelin/APJ system in tumour angiogenesis, using apelin-overexpressing tumour cells. In a human non-small cell lung cancer xenograft model, apelin gene transfer significantly stimulated tumour growth and increased microvessel densities and diameters *in vivo* (*55*). Another group reported that mammary tumour cells stably overexpressing apelin cDNA also stimulated tumour growth *in vivo*, probably associated with enhanced angiogenesis in the tumours (*56*). However, in our own research, we found that overexpression of apelin in colon 26 tumours significantly suppressed tumour growth by inducing tumour vascular maturation (*54*). This difference might depend on the particular apelin/APJ signalling pathway, probably involved in individual tumours and different tumour models, i.e., syngeneic mouse model or allogeneic mouse model using immunodeficient mice. Recent reports indicate that anti-angiogenic cancer drugs, such as VEGF signalling inhibitors, cause 'normalization' of aberrant tumour vasculature and, thus, induce the formation of functional mature vasculature (*57*, *58*). One of the major therapeutic benefits of tumour

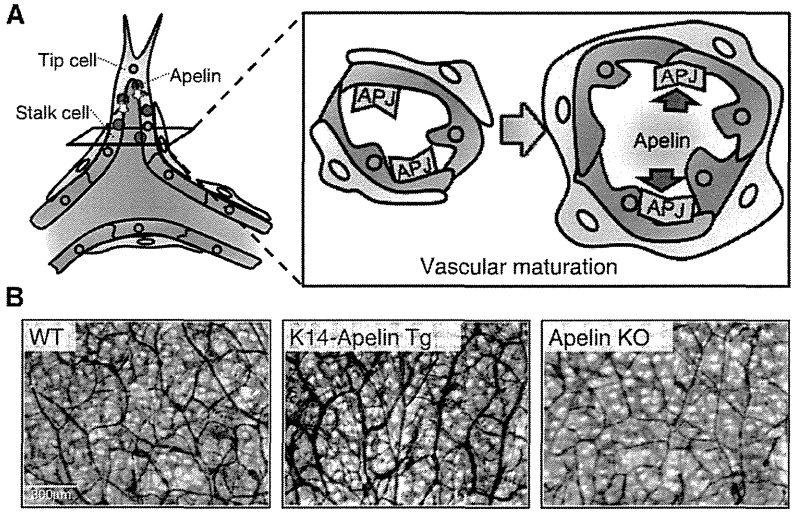

Fig. 2 (A) **Schematic representation showing how apelin/APJ signalling induces vascular maturation.** High levels of expression of apelin protein in tip cells probably activates APJ signalling in the neighbouring stalk cells. Subsequently, these cells will adopt proliferating and aggregating behaviour to form enlarged mature vessels. (B) Image of ear-skin blood vessels in apelin-transgenic mice under regulation of the K14 promoter, and apelin-deficient mice. Compared with wild-type mice, more enlarged mature vessels are observed in apelin-transgenic mice and more narrow immature vessels in apelin-deficient mice.

vascular normalization is enhancement of the effects of conventional anti-tumour therapies, such as chemotherapy and radiation therapy (*58*). In our study, apelin-mediated vascular maturation enhanced the effect of immunotherapy with dendritic cells. These therapeutic effects resulted from induction of tumour cell apoptosis by effective infiltration of activated invariant natural killer T cells (*54*).

Thus, regulation of APJ activity might lead to the development of new vascular normalization drugs, which should be more efficacious than anti-angiogenic agents because of their unique ability to induce vascular enlargement.

Vascular regeneration

Several lines of evidence indicate that apelin can significantly enhance migration, proliferation and capillary tube-like formation of cultured ECs (*30*, *33*, *35*, *44*, *59*). In *in vivo* Matrigel plug assays for angiogenesis, addition of apelin resulted in the formation of capillary-like structures (*33*). Moreover, apelin peptide stimulates angiogenesis in the chicken chorioallantoic membrane assay (*42*). Downregulation of apelin expression by the local delivery of apelin-targeting small interfering RNA into grafted adipose tissue leads to dramatic inhibition of angiogenesis (*59*). In the rat portal hypertension model, treatment with the APJ-specific antagonist F13A markedly reduced splanchnic neovascularization and formation of portosystemic collateral vessels (*60*). According to these reports, it is suggested that apelin can be used for therapeutic angiogenesis.

Analysis of transgenic mice expressing apelin in the epidermis under the transcriptional control of the K14 promoter revealed that apelin can induce the formation of enlarged capillaries, but not arteriola and venula in the dermis. Moreover, overexpression of apelin inhibited vascular leakage caused by VEGF or histamine. These results indicate that apelin can induce non-leaky larger blood vessels *in vivo* (*61*).

In cardiac failure, endothelial apelin expression correlates with other hypoxia-responsive genes, and apelin and APJ are upregulated in ECs of various tissues after systemic hypoxia (10% FIO_2) *in vivo*. It has been suggested that apelin expression in the endothelium of the heart is induced through the endothelial-specific HIF-2α pathway (*62*). Another group also reported that apelin expression was significantly increased in lungs of mice under hypoxic conditions (10% O_2) in an HIF-1α-dependent manner. Small interfering RNA-mediated apelin or APJ knockdown inhibited hypoxia-induced vessel regeneration in the caudal fin regeneration model in zebrafish (*30*). In accordance with these observations, we found that endogenous apelin is required for recovery of hind limb perfusion after induction of ischaemia (*58*). Using mouse hind limb ischaemia models produced by occlusion of the femoral artery, expression of APJ and apelin mRNA was significantly increased in ECs from the ischaemic muscle. In apelin-deficient mice, severe necrosis of the toes and delayed recovery of blood flow were observed when inducing ischaemia. These results suggested the involvement of the apelin/APJ system in collateral vessel formation during the process of recovery from ischaemia states. Thus, we found that APJ expression is induced after ischaemia treatment, and endogenous apelin is required for functional recovery.

Apelin gene transfer promotes formation of enlarged and non-leaky blood vessels in the hind limb ischaemia model. Simultaneous overexpression of apelin and VEGF by plasmid administration was superior to VEGF alone at restoring tissue integrity after ischaemia damage by improved generation of enlarged blood vessels in the ischaemic muscle (*61*). Moreover, apelin

induced vascular stabilization by inhibiting VEGF-mediated internalization of vascular endothelial cadherin resulted in suppression of hind limb oedema (*61*). In addition to its role in blood vessel formation, APJ is expressed in human lymphatic ECs, and apelin induces their migration and cord formation. Transgenic mice harbouring apelin in the dermis showed reduced development of oedema by promoting stabilization of lymphatic vessels (*63*). Taken together, these findings suggest that the apelin/APJ system represents a new therapeutic target for ischaemic disease.

Conclusions

Recent studies have revealed multiple roles of the apelin/APJ system in vascular formation in physiological and pathological situations, including during development, tissue regeneration and tumourigenesis. Apelin has a unique function as a regulator of vascular maturation and stabilization by increasing the caliber of newly formed blood vessels and strengthening barrier function between ECs. Moreover, expression of apelin and APJ genes is temporally upregulated during blood vessel development and downregulated in stabilized vasculature. Detailed understanding of the function of the apelin/APJ system and expression analysis in blood vessels will provide insights for improving the use of agonists and antagonists that modulate apelin signalling in different vascular diseases.

Funding

This work was supported by Grant-in Aid for Scientific Research on Innovative Areas (No. 23122511) from the Ministry of Education, Culture, Sports, Science and Technology (MEXT) and Grant-in Aid for Young Scientist B (No. 23701054) from the Japan Society for the Promotion of Science (JSPS).

Conflict of interest

None declared.

References

1. Tatemoto, K., Hosoya, M., Habata, Y., Fujii, R., Kakegawa, T., Zou, M.X., Kawamata, Y., Fukusumi, S., Hinuma, S., Kitada, C., Kurokawa, T., Onda, H., and Fujino, M. (1998) Isolation and characterization of a novel endogenous peptide ligand for the human APJ receptor. *Biochem. Biophys. Res. Commun.* **251**, 471–476
2. Kawamata, Y., Habata, Y., Fukusumi, S., Hosoya, M., Fujii, R., Hinuma, S., Nishizawa, N., Kitada, C., Onda, H., Nishimura, O., and Fujino, M. (2001) Molecular properties of apelin: tissue distribution and receptor binding. *Biochim. Biophys. Acta.* **1538**, 162–171
3. Masri, B., Lahlou, H., Mazarguil, H., Knibiehler, B., and Audigier, Y. (2002) Apelin (65-77) activates extracellular signal-regulated kinases via a PTX-sensitive G protein. *Biochem. Biophys. Res. Commun.* **290**, 539–545
4. Lee, D.K., Ferguson, S.S., George, S.R., and O'Dowd, B.F. (2010) The fate of the internalized apelin receptor is determined by different isoforms of apelin mediating differential interaction with beta-arrestin. *Biochem. Biophys. Res. Commun.* **395**, 185–189
5. O'Dowd, B.F., Heiber, M., Chan, A., Heng, H.H., Tsui, L.C., Kennedy, J.L., Shi, X., Petronis, A., George, S.R., and Nguyen, T. (1993) A human gene that shows identity with the gene encoding the angiotensin receptor is located on chromosome 11. *Gene* **136**, 355–360
6. Lee, D.K., Cheng, R., Nguyen, T., Fan, T., Kariyawasam, A.P., Liu, Y., Osmond, D.H., George, S.R., and O'Dowd, B.F. (2000) Characterization of apelin, the ligand for the APJ receptor. *J. Neurochem.* **74**, 34–41
7. Tatemoto, K., Takayama, K., Zou, M.X., Kumaki, I., Zhang, W., Kumano, K., and Fujimiya, M. (2001) The novel peptide apelin lowers blood pressure via a nitric oxide-dependent mechanism. *Regul. Pept.* **99**, 87–92
8. Katugampola, S.D., Maguire, J.J., Matthewson, S.R., and Davenport, A.P. (2001) [(125)I]-(Pyr(1))Apelin-13 is a novel radioligand for localizing the APJ orphan receptor in human and rat tissues with evidence for a vasoconstrictor role in man. *Br. J. Pharmacol.* **132**, 1255–1260
9. Foldes, G., Horkay, F., Szokodi, I., Vuolteenaho, O., Ilves, M., Lindstedt, K.A., Mäyränpää, M., Sármán, B., Seres, L., Skoumal, R., Lakó-Futó, Z., deChâtel, R., Ruskoaho, H., and Tóth, M. (2003) Circulating and cardiac levels of apelin, the novel ligand of the orphan receptor APJ, in patients with heart failure. *Biochem. Biophys. Res. Commun.* **308**, 480–485
10. Ronkainen, V.P., Ronkainen, J.J., Hanninen, S.L., Leskinen, H., Ruas, J.L., Pereira, T., Poellinger, L., Vuolteenaho, O., and Tavi, P. (2007) Hypoxia inducible factor regulates the cardiac expression and secretion of apelin. *FASED J.* **21**, 1821–1830
11. Berry, M.F., Pirolli, T.J., Jayasankar, V., Burdick, J., Morine, K.J., Gardner, T.J., and Woo, Y.J. (2004) Apelin has in vivo inotropic effects on normal and failing hearts. *Circulation* **110 (11 Suppl. 1)**, II187–II193
12. Jia, Y.X., Pan, C.S., Zhang, J., Geng, B., Zhao, J., Gerns, H., Yang, J., Chang, J.K., Tang, C.S., and Qi, Y.F. (2006) Apelin protects myocardial injury induced by isoproterenol in rats. *Regul. Pept.* **133**, 147–154
13. Atluri, P., Morine, K.J., Liao, G.P., Panlilio, C.M., Berry, M.F., Hsu, V.M., Hiesinger, W., Cohen, J.E., and Joseph Woo, Y. (2007) Ischemic heart failure enhances endogenous myocardial apelin and APJ receptor expression. *Cell. Mol. Biol. Lett.* **12**, 127–138
14. Maguire, J.J., Kleinz, M.J., Pitkin, S.L., and Davenport, A.P. (2009) [Pyr1]apelin-13 identified as the predominant apelin isoform in the human heart: vasoactive mechanisms and inotropic action in disease. *Hypertension* **54**, 598–604
15. Boucher, J., Masri, B., Daviaud, D., Gesta, S., Guigne, C., Mazzucotelli, A., Castan-Laurell, I., Tack, I., Knibiehler, B., Carpéné, C., Audiqier, Y., Saulnier-Blanche, J.S., and Valet, P. (2005) Apelin, a newly identified adipokine up-regulated by insulin and obesity. *Endocrinology* **146**, 1764–1771
16. Heinonen, M.V., Purhonen, A.K., Miettinen, P., Paakkonen, M., Pirinen, E., Alhava, E., Akerman, K., and Herzig, K.H. (2005) Apelin, orexin-A and leptin plasma levels in morbid obesity and effect of gastric banding. *Regul. Pept.* **130**, 7–13
17. Li, L., Yang, G., Li, Q., Tang, Y., Yang, M., Yang, H., and Li, K. (2006) Changes and relations of circulating visfatin, apelin, and resistin levels in normal, impaired glucose tolerance, and type 2 diabetic subjects. *Exp. Clin. Endocrinol. Diabetes* **114**, 544–548

18. Roberts, E.M., Newson, M.J., Pope, G.R., Landgraf, R., Lolait, S.J., and O'Carroll, A.M. (2009) Abnormal fluid homeostasis in apelin receptor knockout mice. *J. Endocrinol.* **202**, 453–462
19. Lambrecht, N.W., Yakubov, I., Zer, C., and Sachs, G. (2006) Transcriptomes of purified gastric ECL and parietal cells: identification of a novel pathway regulating acid secretion. *Physiol. Genomics* **25**, 153–165
20. Habata, Y., Fujii, R., Hosoya, M., Fukusumi, S., Kawamata, Y., Hinuma, S., Kitada, C., Nishizawa, N., Murosaki, S., Kurokawa, T., Onda, H., Tatemoto, K., and Fujino, M. (1999) Apelin, the natural ligand of the orphan receptor APJ, is abundantly secreted in the colostrum. *Biochim. Biophys. Acta.* **1452**, 25–35
21. Hosoya, M., Kawamata, Y., Fukusumi, S., Fujii, R., Habata, Y., Hinuma, S., Kitada, C., Honda, S., Kurokawa, T., Onda, H., Nishimura, O., and Fujino, M. (2000) Molecular and functional characteristics of APJ. Tissue distribution of mRNA and interaction with the endogenous ligand apelin. *J. Biol. Chem.* **275**, 21061–21067
22. O'Carroll, A.M., Selby, T.L., Palkovits, M., and Lolait, S.J. (2000) Distribution of mRNA encoding B78/apj, the rat homologue of the human APJ receptor, and its endogenous ligand apelin in brain and peripheral tissues. *Biochim. Biophys. Acta.* **1492**, 72–80
23. Devic, E., Rizzoti, K., Bodin, S., Knibiehler, B., and Audigier, Y. (1999) Amino acid sequence and embryonic expression of msr/apj, the mouse homolog of Xenopus X-msr and human APJ. *Mech. Dev.* **84**, 199–203
24. Medhurst, A.D., Jennings, C.A., Robbins, M.J., Davis, R.P., Ellis, C., Winborn, K.Y., Lawrie, K.W., Hervieu, G., Riley, G., Bolaky, J.E., Herrity, N.C., Murdock, P., and Darker, J.G. (2003) Pharmacological and immunohistochemical characterization of the APJ receptor and its endogenous ligand apelin. *J. Neurochem.* **84**, 1162–1172
25. Edinger, A.L., Hoffman, T.L., Sharron, M., Lee, B., Yi, Y., Choe, W., Kolson, D.L., Mitrovic, B., Zhou, Y., Faulds, D., Collman, R.G., Hesselgesser, J., Horuk, R., and Doms, R.W. (1998) An orphan seven-transmembrane domain receptor expressed widely in the brain functions as a coreceptor for human immunodeficiency virus type 1 and simian immunodeficiency virus. *J. Virol.* **72**, 7934–7940
26. Kleinz, M.J. and Davenport, A.P. (2004) Immunocytochemical localization of the endogenous vasoactive peptide apelin to human vascular and endocardial endothelial cells. *Regul. Pept.* **118**, 119–125
27. Wang, G., Qi, X., Wei, W., Englander, E.W., and Greeley, G.H. Jr (2006) Characterization of the 5'-regulatory regions of the rat and human apelin genes and regulation of breast apelin by USF. *FASEB J.* **20**, 2639–2641
28. Han, S., Wang, G., Qi, X., Englander, E.W., and Greeley, G.H. Jr (2008) Involvement of a Stat3 binding site in inflammation-induced enteric apelin expression. *Am. J. Physiol. Gastrointest. Liver Physiol.* **295**, G1068–G1078
29. Mazzucotelli, A., Ribet, C., Castan-Laurell, I., Daviaud, D., Guigne, C., Langin, D., and Valet, P. (2008) The transcriptional co-activator PGC-1alpha up regulates apelin in human and mouse adipocytes. *Regul. Pept.* **150**, 33–37
30. Eyries, M., Siegfried, G., Ciumas, M., Montagne, K., Agrapart, M., Lebrin, F., and Soubrier, F. (2008) Hypoxia-induced apelin expression regulates endothelial cell proliferation and regenerative angiogenesis. *Circ. Res.* **103**, 432–440
31. O'Carroll, A.M., Lolait, S.J., and Howell, G.M. (2006) Transcriptional regulation of the rat apelin receptor gene: promoter cloning and identification of an Sp1 site necessary for promoter activity. *J. Mol. Endocrinol.* **36**, 221–235
32. Hata, J., Matsuda, K., Ninomiya, T., Yonemoto, K., Matsushita, T., Ohnishi, Y., Saito, S., Kitazono, T., Ibayashi, S., Iida, M., Kiyohara, Y., Nakamura, Y., and Kubo, M. (2007) Functional SNP in an Sp1-binding site of AGTRL1 gene is associated with susceptibility to brain infarction. *Hum. Mol. Genet.* **16**, 630–639
33. Kasai, A., Shintani, N., Oda, M., Kakuda, M., Hashimoto, H., Matsuda, T., Hinuma, S., and Baba, A. (2004) Apelin is a novel angiogenic factor in retinal endothelial cells. *Biochem. Biophys. Res. Commun.* **325**, 395–400
34. Hashimoto, Y., Ishida, J., Yamamoto, R., Fujiwara, K., Asada, S., Kasuya, Y., Mochizuki, N., and Fukamizu, A (2005) G protein-coupled APJ receptor signaling induces focal adhesion formation and cell motility. *Int. J. Mol. Med* **16**, 787–792
35. Masri, B., Morin, N., Cornu, M., Knibiehler, B., and Audigier, Y. (2004) Apelin (65-77) activates p70 S6 kinase and is mitogenic for umbilical endothelial cells. *FASEB J.* **18**, 1909–1911
36. Li, Y., Chen, J., Bai, B., Du, H., Liu, Y., and Liu, H. (2012) Heterodimerization of human apelin and kappa opioid receptors: roles in signal transduction. *Cell. Signal.* **24**, 991–1001
37. Alastalo, T.P., Li, M., Perez Vde, J., Pham, D., Sawada, H., Wang, J.K., Koskenvuo, M., Wang, L., Freeman, B.A., Chang, H.Y., and Rabinovitch, M. (2011) Disruption of PPARgamma/beta-catenin-mediated regulation of apelin impairs BMP-induced mouse and human pulmonary arterial EC survival. *J. Clin. Invest.* **121**, 3735–3746
38. Xie, H., Yuan, L.Q., Luo, X.H., Huang, J., Cui, R.R., Guo, L.J., Zhou, H.D., Wu, X.P., and Liao, E.Y. (2007) Apelin suppresses apoptosis of human osteoblasts. *Apoptosis* **12**, 247–254
39. Masri, B., Morin, N., Pedebernade, L., Knibiehler, B., and Audigier, Y. (2006) The apelin receptor is coupled to Gi1 or Gi2 protein and is differentially desensitized by apelin fragments. *J. Biol. Chem.* **281**, 18317–18326
40. Risau, W. (1997) Mechanisms of angiogenesis. *Nature* **386**, 671–674
41. Kalin, R.E., Kretz, M.P., Meyer, A.M., Kispert, A., Heppner, F.L., and Brandli, A.W. (2007) Paracrine and autocrine mechanisms of apelin signaling govern embryonic and tumor angiogenesis. *Dev. Biol.* **305**, 599–614
42. Cox, C.M., D'Agostino, S.L., Miller, M.K., Heimark, R.L., and Krieg, P.A. (2006) Apelin, the ligand for the endothelial G-protein-coupled receptor, APJ, is a potent angiogenic factor required for normal vascular development of the frog embryo. *Dev. Biol.* **296**, 177–189
43. Tucker, B., Hepperle, C., Kortschak, D., Rainbird, B., Wells, S., Oates, A.C., and Lardelli, M. (2007) Zebrafish angiotensin II receptor-like 1a (agtrl1a) is expressed in migrating hypoblast, vasculature, and in multiple embryonic epithelia. *Gene Expr. Patterns* **7**, 258–265
44. Kidoya, H., Ueno, M., Yamada, Y., Mochizuki, N., Nakata, M., Yano, T., Fujii, R., and Takakura, N. (2008) Spatial and temporal role of the apelin/APJ

system in the caliber size regulation of blood vessels during angiogenesis. *EMBO J.* **27**, 522–534

45. Saint-Geniez, M., Masri, B., Malecaze, F., Knibiehler, B., and Audigier, Y. (2002) Expression of the murine msr/apj receptor and its ligand apelin is upregulated during formation of the retinal vessels. *Mech. Dev.* **110**, 183–186
46. Saint-Geniez, M., Argence, C.B., Knibiehler, B., and Audigier, Y. (2003) The msr/apj gene encoding the apelin receptor is an early and specific marker of the venous phenotype in the retinal vasculature. *Gene Expr. Patterns* **3**, 467–472
47. Jakobsson, L., Franco, C.A., Bentley, K., Collins, R.T., Ponsioen, B., Aspalter, I.M., Rosewell, I., Busse, M., Thurston, G., Medvinsky, A., Schuttle-merker, S., and Gerhardt, H. (2010) Endothelial cells dynamically compete for the tip cell position during angiogenic sprouting. *Nat. Cell Biol.* **12**, 943–953
48. Arima, S., Nishiyama, K., Ko, T., Arima, Y., Hakozaki, Y., Sugihara, K., Koseki, H., Uchijima, Y., Kurihara, Y., and Kurihara, H. (2011) Angiogenic morphogenesis driven by dynamic and heterogeneous collective endothelial cell movement. *Development* **138**, 4763–4776
49. del Toro, R., Prahst, C., Mathivet, T., Siegfried, G., Kaminker, J.S., Larrivee, B., Breant, C., Duarte, A., Takakura, N., Fukamizu, A., Penninger, J., and Eichmann, A. (2010) Identification and functional analysis of endothelial tip cell-enriched genes. *Blood* **116**, 4025–4033
50. Kasai, A., Shintani, N., Kato, H., Matsuda, S., Gomi, F., Haba, R., Hashimoto, H., Kakuda, M., Tano, Y., and Baba, A. (2008) Retardation of retinal vascular development in apelin-deficient mice. *Arterioscler. Thromb. Vasc. Biol.* **28**, 1717–1722
51. Sakimoto, S., Kidoya, H., Naito, H., Kamei, M., Sakaguchi, H., Goda, N., Fukamizu, A., Nishida, K., and Takakura, N. (2012) A role for endothelial cells in promoting the maturation of astrocytes through the apelin/APJ system in mice. *Development* **139**, 1327–1335
52. Seaman, S., Stevens, J., Yang, M.Y., Logsdon, D., Graff-Cherry, C., and St Croix, B. (2007) Genes that distinguish physiological and pathological angiogenesis. *Cancer Cell* **11**, 539–554
53. Wang, Z., Greeley, G.H. Jr, and Qiu, S. (2008) Immunohistochemical localization of apelin in human normal breast and breast carcinoma. *J. Mol. Histol.* **39**, 121–124
54. Kidoya, H., Kunii, N., Naito, H., Muramatsu, F., Okamoto, Y., Nakayama, T., and Takakura, N. (2011) The apelin/APJ system induces maturation of the tumor vasculature and improves the efficiency of immune therapy. *Oncogene*, doi: 10.1038/onc.2011.489
55. Berta, J., Kenessey, I., Dobos, J., Tovari, J., Klepetko, W., Jan Ankersmit, H., Hegedus, B., Renyi-Vamos, F., Varga, J., Lorincz, Z., Paku, S., Ostoros, G., Rozsas, A., Timar, J., and Dome, B. (2010) Apelin expression in human non-small cell lung cancer: role in angiogenesis and prognosis. *J. Thorac. Oncol.* **5**, 1120–1129
56. Sorli, S.C., Le Gonidec, S., Knibiehler, B., and Audigier, Y. (2007) Apelin is a potent activator of tumour neoangiogenesis. *Oncogene* **26**, 7692–7699
57. Jain, R.K. (2005) Normalization of tumor vasculature: an emerging concept in antiangiogenic therapy. *Science* **307**, 58–62
58. Dickson, P.V., Hamner, J.B., Sims, T.L., Fraga, C.H., Ng, C.Y., Rajasekeran, S., Hagedorn, N.L., McCarville, M.B., Stewart, C.F., and Davidoff, A.M. (2007) Bevacizumab-induced transient remodeling of the vasculature in neuroblastoma xenografts results in improved delivery and efficacy of systemically administered chemotherapy. *Clin. Cancer Res.* **13**, 3942–3950
59. Kunduzova, O., Alet, N., Delesque-Touchard, N., Millet, L., Castan-Laurell, I., Muller, C., Dray, C., Schaeffer, P., Herault, J.P., Savi, P., Bono, F., and Valet, P. (2008) Apelin/APJ signaling system: a potential link between adipose tissue and endothelial angiogenic processes. *FASEB J.* **22**, 4146–4153
60. Tiani, C., Garcia-Pras, E., Mejias, M., de Gottardi, A., Berzigotti, A., Bosch, J., and Fernandez, M. (2009) Apelin signaling modulates splanchnic angiogenesis and portosystemic collateral vessel formation in rats with portal hypertension. *J. Hepatol.* **50**, 296–305
61. Kidoya, H., Naito, H., and Takakura, N. (2010) Apelin induces enlarged and nonleaky blood vessels for functional recovery from ischemia. *Blood* **115**, 3166–3174
62. Sheikh, A.Y., Chun, H.J., Glassford, A.J., Kundu, R.K., Kutschka, I., Ardigo, D., Hendry, S.L., Wagner, R.A., Chen, M.M., Ali, Z.A., Yue, P., Huynh, D.T., Connolly, A.J., Pelletier, M.P., Tsao, P.S., Robbins, R.C., and Quertermous, T. (2008) In vivo genetic profiling and cellular localization of apelin reveals a hypoxia-sensitive, endothelial-centered pathway activated in ischemic heart failure. *Am. J. Physiol. Heart Circ. Physiol.* **294**, H88–H98
63. Sawane, M., Kidoya, H., Muramatsu, F., Takakura, N., and Kajiya, K Apelin attenuates UVB-induced edema and inflammation by promoting vessel function. *Am. J. Pathol* **179**, 2691–2697

Development 139, 1327-1335 (2012) doi:10.1242/dev.072330

A role for endothelial cells in promoting the maturation of astrocytes through the apelin/APJ system in mice

Susumu Sakimoto[1,2], Hiroyasu Kidoya[1], Hisamichi Naito[1], Motohiro Kamei[2], Hirokazu Sakaguchi[2], Nobuhito Goda[4], Akiyoshi Fukamizu[3], Kohji Nishida[2] and Nobuyuki Takakura[1,5,*]

SUMMARY

Interactions between astrocytes and endothelial cells (ECs) are crucial for retinal vascular formation. Astrocytes induce migration and proliferation of ECs via their production of vascular endothelial growth factor (VEGF) and, conversely, ECs induce maturation of astrocytes possibly by the secretion of leukemia inhibitory factor (LIF). Together with the maturation of astrocytes, this finalizes angiogenesis. Thus far, the mechanisms triggering LIF production in ECs are unclear. Here we show that apelin, a ligand for the endothelial receptor APJ, induces maturation of astrocytes mediated by the production of LIF from ECs. *APJ* (*Aplnr*)- and *Apln*-deficient mice show delayed angiogenesis; however, aberrant overgrowth of endothelial networks with immature astrocyte overgrowth was induced. When ECs were stimulated with apelin, LIF expression was upregulated and intraocular injection of LIF into *APJ*-deficient mice suppressed EC and astrocyte overgrowth. These data suggest an involvement of apelin/APJ in the maturation process of retinal angiogenesis.

KEY WORDS: Astrocytes, Endothelial cells, Apelin, Mouse

INTRODUCTION

The retina is composed of several cell types. Interactions between endothelial cells (ECs), astrocytes and neuronal cells is crucial for fine capillary network formation by ECs. Before the onset of interactions between ECs and astrocytes in the retina of postnatal mice, astrocytes invade from the optic nerve head via the axons of retinal ganglion cells. Controlling this association between different cell components, platelet-derived growth factor A (PDGFA) from retinal ganglion cells promotes growth of immature astrocytes expressing PDGF receptor α (PDGFRα). This results in astrocyte network formation (Fruttiger et al., 1996). Subsequently, ECs from the optic nerve head invade and migrate over the network-forming astrocytes as a template. A crucial role of vascular endothelial growth factor (VEGF), produced by astrocytes, in guiding endothelial tip cells in the vascular branch and in the proliferation of endothelial stalk cells behind the tip cells has been reported (Gerhardt et al., 2003).

In the course of retinal angiogenesis, astrocytes act as proangiogenic accessory cells, as described above; however, upon becoming overlaid with ECs, it has been suggested that their proangiogenic activity ceases and they instead stabilize newly developed blood vessels (West et al., 2005; Kubota et al., 2008). Anatomical analysis has revealed that astrocytes expressing low levels of glial fibrillary acidic protein (GFAP) firstly invade the retina, gradually express higher levels of GFAP, and become quiescent (Chu et al., 2001; Gariano, 2003). Therefore, it has been suggested that ECs might change astrocyte characteristics (Zhang and Stone, 1997), with several lines of evidence suggesting that leukemia inhibitory factor (LIF) derived from ECs is a direct maturation factor for immature astrocytes in vitro (Mi et al., 2001) and in vivo (Kubota et al., 2008). However, the mechanism responsible for controlling LIF production by ECs for maturation of astrocytes has not been elucidated.

During the process of angiogenesis, maturation of blood vessels is induced by angiopoietin 1 (ANG1; also known as ANGPT1), a ligand for endothelial receptor tyrosine kinase TIE2 (also known as TEK), produced by mural cells, which directly adhere to ECs. This results in structural stabilization of the blood vessels (Sato et al., 1995; Suri et al., 1996; Augustin et al., 2009). Apelin is a ligand for the G protein-coupled receptor APJ expressed on ECs. We previously reported that activation of TIE2 promotes apelin production from ECs and that ANG1/TIE2-mediated maturation of blood vessels, such as their enlargement and non-leaky blood vessel formation, is partly dependent on APJ activation by apelin ligation (Kidoya et al., 2008; Kidoya et al., 2010). Recently, involvement of the apelin/APJ system in retinal angiogenesis has been reported (Kasai et al., 2008; del Toro et al., 2010) in which delayed angiogenesis and reduced proliferation of stalk cells was observed in gene ablation analysis of apelin (*Apln*) and apelin receptor (*APJ*; *Aplnr* – Mouse Genome Informatics) (Kasai et al., 2008; del Toro et al., 2010; Kidoya et al., 2010). In contrast to the constitutive expression of TIE2, as well as of VEGF receptor 2 (VEGFR2; also known as FLK1 and KDR), APJ expression in ECs is transient. From the onset of retinal angiogenesis, most network-forming ECs express APJ until postnatal day (P) 7; however, after reaching the marginal zone of the retina, ECs stop expressing APJ at P12, except for the larger veins (Saint-Geniez et al., 2003). Taken together, these findings imply that apelin/APJ acts as a maturation factor for newly developed blood vessels, in addition to its proangiogenic function.

During retinal angiogenesis, it is suggested that ECs and astrocytes mature simultaneously in a mutually dependent manner. However, whether maturation arrest of blood vessels affects

[1]Department of Signal Transduction, Research Institute for Microbial Diseases, Osaka University, 3-1 Yamada-oka, Suita, Osaka 565-0871, Japan. [2]Department of Ophthalmology, Osaka University Graduate School of Medicine, Suita, Osaka 565-0871, Japan. [3]Center for Tsukuba Advanced Research Alliance, Institute of Applied Biochemistry, University of Tsukuba, Ibaraki 305-8577, Japan. [4]Department of Life Science and Medical Bio-Science, School of Advanced Science and Engineering, Waseda University, 2-2 Wakamatsu-cho, Shinjuku-ku, Tokyo 162-8480, Japan. [5]JST, CREST, K's Gobancho, 7 Gobancho, Chiyoda-ku, Tokyo 102-0076, Japan.

*Author for correspondence (ntakaku@biken.osaka-u.ac.jp)

Accepted 15 January 2012

astrocyte maturation is not yet clear. Because apelin/APJ is mainly involved in the maturation of blood vessels, we used mice with *Apln* as well as *APJ* mutations to ask whether the maturation of astrocytes is affected by a deficiency of apelin or APJ. Moreover, we investigated how astrocyte maturation conversely affects the growth of ECs in order to understand mutual EC/astrocyte regulation.

MATERIALS AND METHODS

Mice

All experiments were carried out under the guidelines of the Osaka University Committee for Animal Research. C57BL/6 (Japan SLC, Shizuoka, Japan), *APJ* knockout (KO) (Ishida et al., 2004) and *Apln* KO (Kidoya et al., 2008) mice were used in these studies. Animals were housed in environmentally controlled rooms of the animal experimentation facility at Osaka University.

Quantitative reverse transcription real-time PCR (qRT-PCR)

Total RNA was extracted from cells and tissues using the RNeasy Plus Mini Kit (Qiagen) and transcribed into cDNA using the ExScript RT Reagent Kit (Takara) according to the manufacturers' protocols. Real-time PCR analysis was performed using Platinum SYBR Green qPCR SuperMix-UDG (Invitrogen) and an Mx3000P QPCR System (Stratagene). The baseline and threshold were adjusted according to the manufacturer's instructions. PCR was performed on cDNA using the primers listed in supplementary material Table S1. The level of expression of the target gene was normalized to that of *Gapdh* in each sample.

Tissue immunostaining and in situ hybridization (ISH)

Tissue preparation and staining were as previously reported (Takakura et al., 2000). Enucleated eyes were fixed in 4% paraformaldehyde. Antibodies for staining were anti-PECAM1 (BD Biosciences, 1:100; or Chemicon International, 1:100), anti-GFAP (Sigma-Aldrich, 1:100), anti-PDGFRα (eBioscience, 1:100), anti-desmin (DAKO, 1:100), anti-PAX2 (Covance, 1:100), anti-KI67 (DAKO, 1:100), anti-neurofilament (American Research Products, 1:100), anti-type IV collagen (Cosmo Bio, 1:100), anti-HIF1α (1:100) (Kurihara et al., 2010), anti-apelin (1:100) (Kidoya et al., 2008) and anti-APJ (1:100) (Kidoya et al., 2008). The secondary antibodies used were Alexa Fluor 488/546/647-conjugated IgGs (Invitrogen, 1:200) or FITC/Cy5-conjugated IgGs (Jackson ImmunoResearch Laboratories, 1:200).

For whole-mount ISH, retinas were briefly digested with proteinase K and hybridized with digoxigenin-labeled antisense RNA probes.

For determination of hypoxic tissue, mice were injected intraperitoneally with 60 mg/kg body weight Hypoxyprobe-1 (pimonidazole hydrochloride) (Natural Pharmacia International) before harvesting retinas for tissue processing and staining according to the manufacturer's instructions. Six animals per group were analyzed. A total of eight straight lines were drawn in each retina: four from the optic nerve to the vascular front representing a vascularized area; and four from the vascular front to the peripheral retina as an avascular area. Samples were visualized using conventional microscopy (with a DM5500B equipped with HCX PL FLVOTAR 5/0.15 and HCX PL FLVOTAR 0/0.15 dry objective lenses, Leica) or confocal microscopy (TCS/SP5 equipped with HC PLAN APO 2/0.70 and HCXPL APO 4/1.25-0.75 oil objective lenses, Leica) at room temperature. Images were acquired with a DFC 500 digital camera (Leica) and processed with the Leica application suite and Adobe Photoshop CS3 software. All images shown are representative of three to six independent experiments.

Retina quantification

Complete high-resolution three-dimensional (3D) rendering of whole-mount retinas was achieved using the confocal microscope described above. The cells of interest ($PAX2^+$ astrocytes, $PAX2^+$ $KI67^+$ astrocytes and $HIF1\alpha^+$ cells) were manually scored in six random 350×350 μm or 250×250 μm ($HIF1\alpha^+$ cells) fields of view (FOV) per retina photographed at 40× or 63× magnification using the software of the Leica application suite. To determine cell number and measure the capillary density of the retinas, six animals per group were analyzed. After conversion to 8-bit grayscale using ImageJ software, the capillary density in the vascularized area was quantified from the pixels. The vascularized areas were defined as the region near the vascular front without the regions from the very tips to the first vascular loop. The avascular areas were defined as the regions ~500 μm ahead of the vascular front. $HIF1\alpha^+$ cells were counted in different areas.

Flow cytometry analysis

Retinas of at least five WT and *APJ* KO mouse neonates were incubated for 30 minutes at 37°C in DMEM containing 1% collagenase (Wako, Osaka, Japan) before cells were dissociated by gentle trituration. Cells were pretreated with Fc-Blocker (BD Biosciences Pharmingen) and stained with FITC-conjugated anti-CD140a (PDGFRα) monoclonal antibody and phycoerythrin-conjugated anti-CD31 monoclonal antibody (BD Biosciences Pharmingen). Procedures for cell preparation and staining were as previously reported (Kidoya et al., 2008). The stained cells were analyzed and sorted using a FACSAria flow cytometer (BD) with FlowJo (TreeStar) or CellQuest (BD) software. Dead cells were excluded from the analyses using the 2D profile of forward versus side scatter. Using these negative and positive control tubes, we set fluorescence voltages and the compensation matrix according to the instructions of the manufacturer. We applied these setting parameters to all samples analyzed.

Intraocular injection

Sterile PBS with or without 1 mg/ml apelin (Bachem), 0.5 mg/ml LIF (ESGRO, Chemicon) or 1 mg/ml sFLT1 was injected into the vitreous humor of P3 mice using a sterile injection capillary with an automatic microinjector (FemtoJet, Eppendorf). Mice were sacrificed 48 hours later and the retinas isolated for cell purification or immunohistochemistry.

Cell culture

The mouse microvascular endothelial cell line bEnd.3 or HUVECs were cultured in six-well plates for 12 hours in DMEM or Humedia EG2 (Kurabo, Osaka, Japan), respectively. Cells were then incubated in medium supplemented with 1% fetal bovine serum (FBS). After 6 hours of serum deprivation, cells were stimulated with basal medium containing 20 ng/ml VEGFA 165 (PeproTech) for 18 hours and subsequently incubated with 50 or 500 ng/ml apelin. Culturing of retinal cells was performed as described previously (West et al., 2005). P1 WT retinas were dissected as indicated above, redissociated in DMEM containing 10% FBS and then plated on poly-D-lysine-coated coverslips in 24-well plates at 1.5×10^6 cells/well and incubated at 37°C, 5% CO_2 for 24 hours. Retinal cells were incubated for 24 hours with supernatant of bEnd.3 cells that had been treated with apelin for 24 hours.

Statistical analysis

Data are presented as mean±s.d. for the in vitro studies and mean±s.e. for in vivo studies. For statistical analysis, the Statcel 2 software package (OMS) was used with analysis of variance performed on all data followed by Tukey-Kramer multiple comparison testing. When only two groups were compared, a two-sided Student's *t*-test was used. $P<0.05$ was considered statistically significant.

RESULTS

Dense astrocyte network formation is induced in APJ-deficient mice

Because it has been reported that *APJ* mutant mice show retarded endothelial network formation in the retina (del Toro et al., 2010), we first investigated the development of, and network formation by, astrocytes from P0 to P7 (Fig. 1A). Using anti-PDGFRα antibody in immunohistochemistry (IHC) to identify these cells, we found that astrocyte network formation was similar in wild-type (WT) and *APJ* KO mice at P1; however, a dense network appeared in *APJ* KO mice at P5 and continued at least until P7. $PDGFR\alpha^+$ astrocytes were also analyzed by flow cytometry and their number calculated as a proportion of the total number of retinal cells at P5. A significantly greater proportion of astrocytes was found to be present in *APJ* KO

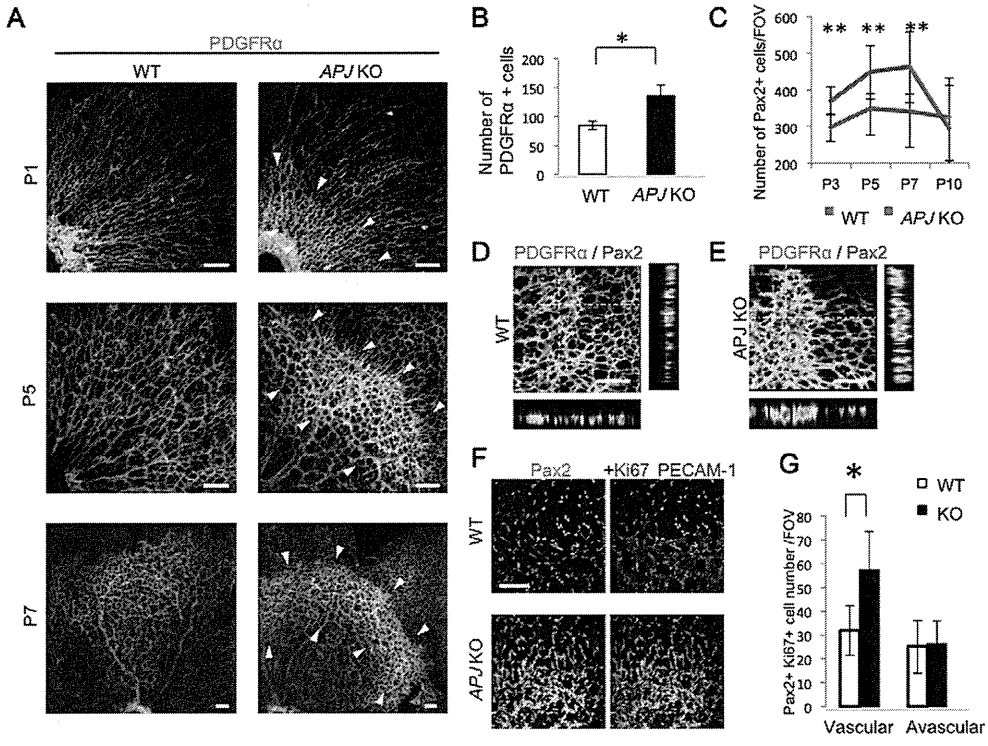

Fig. 1. *APJ* KO mice show irregular remodeling and proliferation of retinal astrocytes. (**A**) Immunohistochemistry (IHC) for PDGFRα (green) in the P1, P5 and P7 developing retina of wild-type (WT) or *APJ* KO mice. Note the dense astrocyte network (surrounded by arrowheads) in *APJ* KO mice. (**B**) Quantitative evaluation of the number of PDGFRα$^+$ cells per 5×10^4 cells analyzed by FACS. Dissociated retinal cells from P5 WT or *APJ* KO mice were used (n=4, *P<0.05). (**C**) Transition of the number of astrocytes identified as PAX2$^+$ nuclei in vascularized areas. Data are the mean of six random fields of view (FOV) in the vascularized area per retina (n=6, **P<0.01). (**D**,**E**) Confocal microscopy images of PDGFRα$^+$ (green) and PAX2$^+$ (red) astrocytes in WT (D) and *APJ* KO (E) P5 retinas. z-stack images show two-layered astrocytes in *APJ* KO retina. (**F**) Proliferation status of astrocytes in P5 retinas from WT and *APJ* KO mice. Retinas were stained with antibodies against PAX2 (green), KI67 (magenta) and PECAM1 (blue). Note the marked proliferation of PAX2$^+$ KI67$^+$ astrocytes (white or light blue) in vascular areas of *APJ* KO mice. (**G**) Quantification of PAX2$^+$ KI67$^+$ astrocytes in the vascularized or non-vascularized retinal areas. Six random FOV were examined per retina (n=6,*P<0.05). Error bars indicate s.d. Scale bars: 100 μm.

than WT mice (Fig. 1B). We next calculated the number of astrocytes expressing PAX2, a nuclear transcription factor present in all cells of the astrocyte lineage (Fig. 1C-E). Although the number of PAX2$^+$ astrocytes in *APJ* KO mice was higher than in WT mice from P3 to P7, it gradually decreased to WT levels, suggesting negative-feedback regulation (Fig. 1C). z-stack images suggested that a thicker retinal astrocyte layer was induced in *APJ* KO than in WT mice owing to the generation of two layers of astrocytes at P5 (Fig. 1D,E). Next, we stained the retina for the EC marker PECAM1 (CD31) and with anti-PAX2 antibody, as well as for the cell proliferation marker (KI67). High-density areas of PAX2$^+$ KI67$^+$ proliferating astrocytes were present in vascular but not avascular areas (Fig. 1F,G), suggesting that astrocyte proliferation is associated with ECs.

Next we assessed the degree of astrocyte maturation in *APJ* KO mice. In WT mice, astrocytes that are initially weakly GFAP positive start to express a high level of GFAP at P5 (Fig. 2A-C). The strongly GFAP-positive astrocytes present from the optic nerve head up to the beginning of the dense astrocyte sheet area did not differ substantially between *APJ* KO and WT mice. However, within the dense astrocyte sheet there were fewer strongly GFAP-positive astrocytes in the *APJ* KO mice (Fig. 2A,D,E). Consistent with this, levels of *Gfap* mRNA were reduced in *APJ* KO mice at all periods examined (Fig. 2F). Comparing other astrocyte differentiation markers in *APJ* KO and WT mice revealed similar levels of expression for the lineage markers vimentin (*Vim*) and *Pax2* but a significant reduction in the mature astrocyte markers *S100b* and *Gfap* in the knockouts (Fig. 2G). These data suggest that APJ deficiency does not affect the development of astrocytes but influences their maturation.

APJ deficiency indirectly induces dense endothelial sheets via overgrowth of immature astrocytes

It has been reported that both *APJ* KO and *Apln* KO mice show delayed retinal angiogenesis (Kasai et al., 2008; del Toro et al., 2010). However, as we found aberrant overgrowth of immature astrocytes in *APJ* KO mice, we hypothesized that abnormal overgrowth during blood vessel formation should also be induced in *APJ* KO mice indirectly owing to the defect of APJ in ECs, as weakly GFAP-positive astrocytes possess proangiogenic properties. Although retinal vessel outgrowth from the optic nerve head was indeed impaired in *APJ* KO mice (supplementary material Fig. S1) as previously reported (del Toro et al., 2010), a dense endothelial network-forming area was frequently observed at the migrating front of the retinal vasculature after P5 (Fig. 3A-C).

Consistent with hyperproliferation of ECs in *APJ* KO mice, the retinas of these mice were found by in situ hybridization (ISH) to express more *Vegfa* mRNA in the peripheral region of

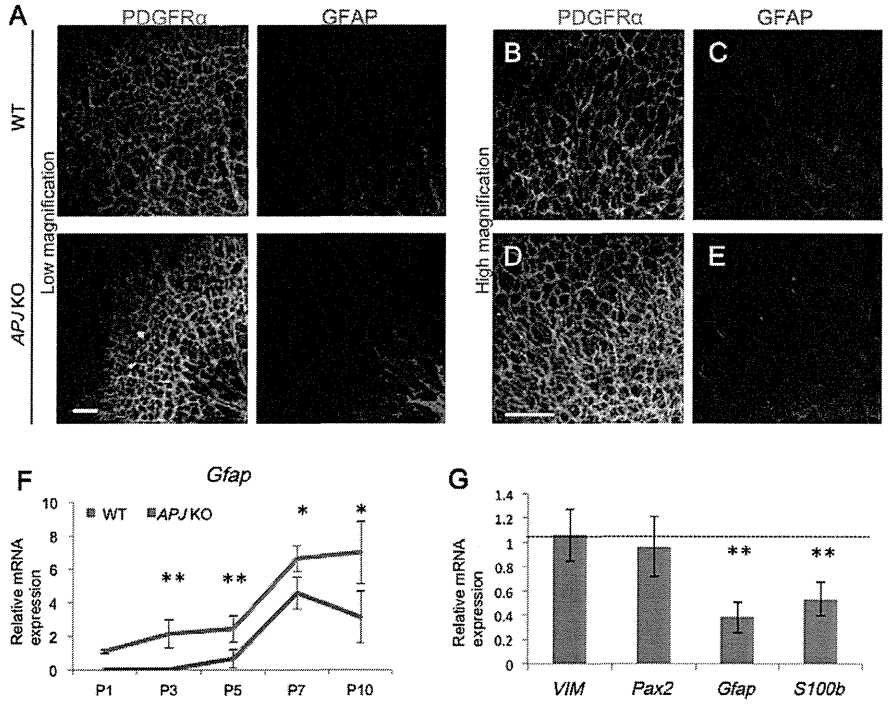

Fig. 2. Suppression of astrocyte maturation in *APJ* KO developing retina. (**A**) Retinal astrocytes stained for PDGFRα (green) and GFAP (red) in P5 WT and *APJ* KO mice. (**B-E**) High-magnification views of retinal astrocytes around the migrating front of the vascular network area as shown in Fig. 1F. Note the weak positivity for GFAP in overgrown astrocytes in *APJ* KO mice. (**F**) Quantitative RT-PCR (qPCR) analysis of *Gfap* expression using isolated RNA from FACS-sorted PDGFRα$^+$ cells at various retinal stages (n=3, *P<0.05, **P<0.01). (**G**) qPCR analysis of retinal astrocyte marker expression with RNA isolated from sorted PDGFRα$^+$ cells of P5 retina. Data represent relative mRNA expression from *APJ* KO mice as compared with WT mice set as unity (n=3, **P<0.01). Dotted line indicates level of WT. Error bars indicate s.d. Scale bars: 100 μm.

the endothelial network-forming area than did WT mice at P5 (Fig. 3D). Moreover, comparing sorted retinal PDGFRα$^+$ astrocytes revealed greater *Vegfa* mRNA expression in *APJ* KO than in WT mice (Fig. 3E). VEGF expression is known to be regulated by hypoxia via hypoxia inducible factor 1α (HIF1α). It has been reported that suppression of retinal vascular growth by VEGF-Trap injections primarily leads to VEGF upregulation, GFAP downregulation, and dense network formation in retinal astrocytes (Uemura et al., 2006). Moreover, West et al. have clearly demonstrated that hypoxia inhibits the maturation of astrocytes, resulting in VEGF upregulation, using models for retinopathy of prematurity (West et al., 2005). Currently, it is widely accepted that hypoxia is crucial for the regulation of astrocyte maturation. Therefore, it is possible that the hyperproliferation of ECs observed in *APJ* KO mice is caused by hypoxia induced by impaired vessel outgrowth. Indeed, compared with WT mice, slightly stronger Hypoxyprobe-1 signals were observed in the avascular area of the vascular front (asterisks in Fig. 4A,B) and the hypovascular areas in the middle of the vascular network (the areas enclosed by the dashed lines in Fig. 4A) in *APJ* KO mice. Although the levels of *Hif1a* mRNA were not significantly different in the whole retinas of WT and *APJ* KO mice (supplementary material Fig. S3), nuclear translocation of HIF1α, indicating its state of activation, was

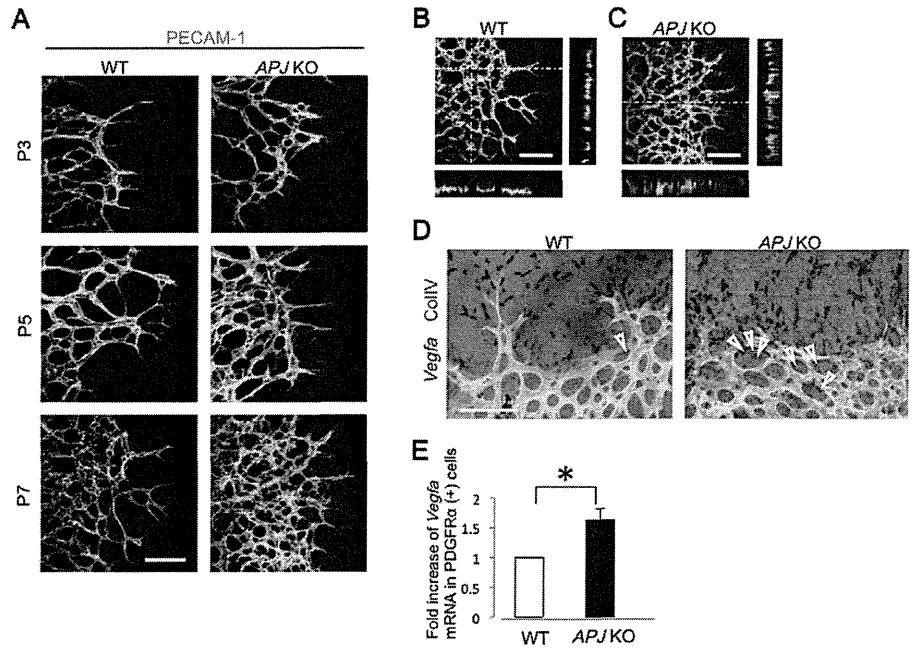

Fig. 3. Aberrant overgrowth of ECs in *APJ* KO mice. (**A**) Whole-mount anti-PECAM1 immunostaining of the developing retina around the vascular front of P3, P5 and P7 WT and *APJ* KO mice. (**B,C**) Confocal microscopy images of PECAM1$^+$ ECs in P7 WT (B) and *APJ* KO (C) mouse retinas. *z*-stack images show a denser EC layer in *APJ* KO than in WT retina. (**D**) In situ hybridization (ISH) for *Vegfa* combined with IHC for collagen IV in the vascular front. Note the increase of *Vegfa* mRNA in *APJ* KO retina. Arrowheads indicate upregulation of *Vegfa* mRNA even in the vascular area. (**E**) qPCR analysis of *Vegfa* mRNA expression in retinal PDGFRα$^+$ astrocytes from P5 retinas of WT and *APJ* KO mice (n=3, *P<0.05). Error bars indicate s.d. Scale bars: 100 μm.

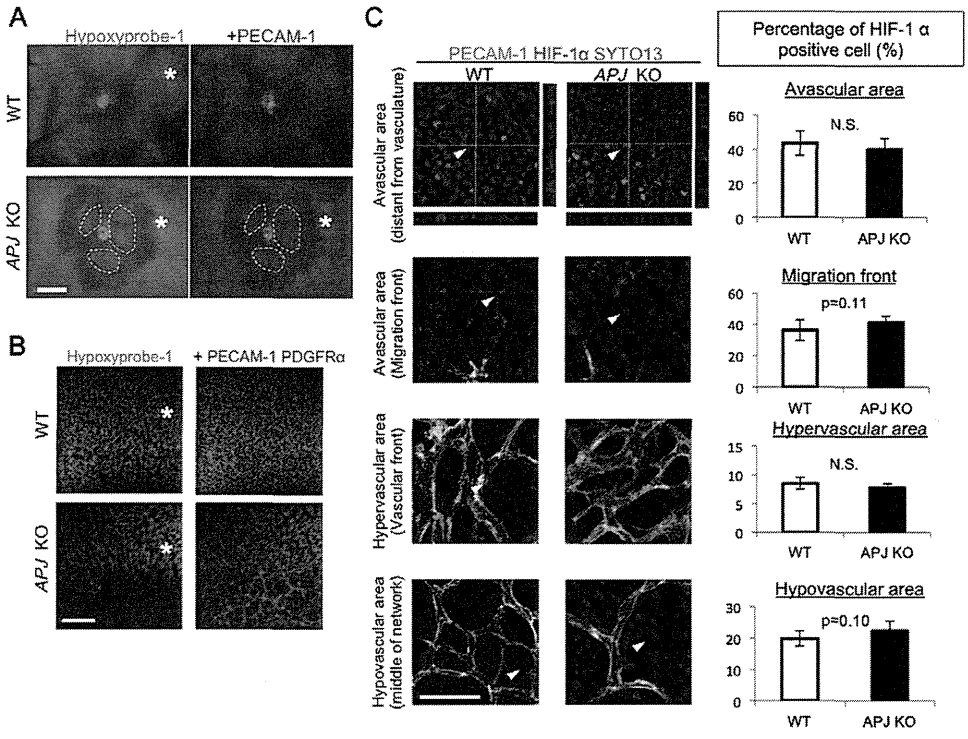

Fig. 4. Evaluation of hypoxic status in *APJ* KO mice. (**A**) Low-magnification images of hypoxic status in *APJ* KO mouse retina. Detection of PECAM1 (red) and Hypoxyprobe-1 (green) in P5 WT and *APJ* KO retinas. Asterisks indicate avascular areas of the vascular front and the areas demarcated by dashed lines indicate the hypovascular areas in the middle of the vascular network. (**B**) Higher magnification images of hypoxic status showing PECAM1 (red), PDGFRα (blue) and Hypoxyprobe-1 (green) in P5 WT and *APJ* KO retinas. (**C**) Nuclear translocation of HIF1α protein in *APJ* KO mice. Retinas of WT and *APJ* KO mice were dissected at P5 and whole-mount immunostaining was performed using anti-PECAM1 (green) and anti-HIF1α (red) antibodies and analyzed in different areas. Arrowheads indicate nuclear positivity for HIF1α. *z*-stack image showing localization of HIF1α in nuclei stained with SYTO13 (blue). (Right) Percentages of nuclear HIF1α$^+$ cells in the areas described were quantitatively evaluated. Four random FOV in the vascularized area were examined per retina (n=6). N.S., not significant. Error bars indicate s.d. Scale bars: 500 μm in A; 100 μm in B; 50 μm in C.

slightly enhanced in areas where more intense Hypoxyprobe-1 signals were observed in the *APJ* KO mice (Fig. 4C). However, the difference in HIFα nuclear translocation in WT and *APJ* KO mice was not statistically significant.

These data suggest that the VEGFA overexpression observed in astrocytes from *APJ* KO mice and the partial dense vascular network formation are dependent on hypoxia as a primary effect of APJ deficiency. However, compared with other models using VEGF-Trap (Uemura et al., 2006) or retinopathy of prematurity (West et al., 2005), in which blood vessel formation in the retina is completely abolished and strong hypoxia is induced, the degree of vascular defects and hypoxia observed here in *APJ* KO mice was not severe. Therefore, we consider that not only hypoxia but also other mechanisms underlie the maturation of astrocytes affected by APJ.

It is possible that APJ is expressed on astrocytes and that this, rather than its absence from ECs, affects the growth of immature astrocytes directly. However, we were unable to detect APJ expression on PDGFRα$^+$ astrocytes, whereas it was present on ECs (supplementary material Fig. S2). Moreover, we assessed whether the overgrowth of astrocytes is affected by aberrant growth of retinal ganglion cells. As shown in Fig. 5A, radially migrated well-organized retinal ganglion cells were present in *APJ* KO mice to the same extent as in WT mice. Expression of *Pdgfa* mRNA in retinal tissue was not increased in *APJ* KO mice relative to WT mice (Fig. 5B).

Next, we tested whether moderate, but not severely, delayed angiogenesis in the retina, as observed in *APJ* KO mice, affects astrocyte proliferation in WT mice by neutralizing VEGF using injections of soluble (s) FLT1 (VEGFR1). We started to neutralize VEGF from P3 and assessed its effects on vascular formation at P5, as severe vascular defects were induced when VEGF was neutralized from P0, as previously reported (Uemura et al., 2006). As shown in Fig. 5C, treatment with sFLT1 according to this schedule retarded the outgrowth of blood vessels to a similar extent to that observed in *APJ* KO mice. Although a partial dense astrocyte sheet was observed (Fig. 5C, arrow), *z*-stack images suggested that the thickness of the astrocyte layer was almost the same in PBS-treated or sFLT1-treated mice (Fig. 5D). Furthermore, increases in the total number and proliferation of astrocytes were not observed (Fig. 5E-H). These data suggest that molecular cues that are absent owing to the lack of APJ in ECs affect overgrowth by immature astrocytes.

Exogenous apelin induces the expression of GFAP in retinal astrocytes

Based on this result that a lack of APJ on ECs affects the outgrowth of immature astrocytes, we next examined whether apelin is involved in astrocyte differentiation and proliferation in vivo. Immunohistochemical analysis revealed that GFAP expression on astrocytes at P5 was enhanced following intraocular injection of apelin into WT mice at P3 (Fig. 6A). We confirmed upregulation

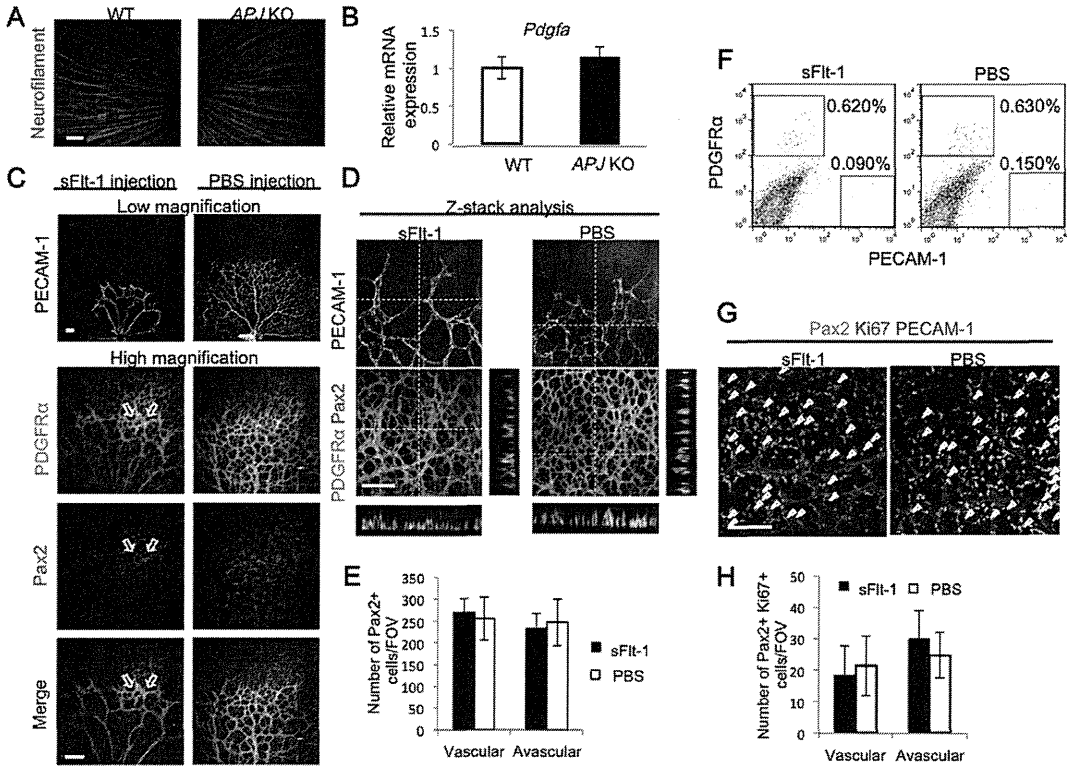

Fig. 5. Evaluation of neuronal cell development in the absence of APJ and its effects on proliferation of astrocytes mediated by retardation of vascular development. (**A**) The morphology of retinal ganglion cells in P3 WT and *APJ* KO mouse retinas. Retinas were stained with anti-neurofilament antibody. (**B**) qPCR analysis of *Pdgfa* mRNA expression in P5 WT and *APJ* KO retinas. (**C-G**) Effect of vascular retardation on astrocyte development in the retina assessed by intraocular injection of soluble (s) FLT1 or PBS (control). (C) Retinas were stained with antibodies against PDGFRα (green), PAX2 (red) and PECAM1 (white) at P5, 48 hours after treatment with sFLT1 or PBS. Although sFLT1 retarded vascular outgrowth, this degree of vascular defectiveness did not induce substantially abnormal networks of astrocytes at the vascular front with the exception of slight dense astrocyte network formation (arrows in C). (D) *z*-stack imaging showing no differences in the thickness of the glial cell layer or in the number of PAX2$^+$ cells between PBS- and sFLT1-treated mice. (E) Quantification of PAX2$^+$ astrocytes in the vascular and avascular areas. (F) Flow cytometry analysis of P5 retina from PBS- and sFLT1-treated mice (n=8). The number of PECAM1$^+$ cells decreased with sFLT1 treatment but the number of PDGFRα$^+$ cells did not change. (G) Proliferation status of astrocytes in P5 retinas from PBS- and sFLT1-treated mice. Retinas were stained with antibodies against PAX2 (green), KI67 (magenta) and PECAM1 (blue). Arrowheads indicate PAX2$^+$ KI67$^+$ astrocytes in vascular areas of P5 retinas from PBS- and sFLT1-treated mice. (**H**) Quantification of PAX2$^+$ KI67$^+$ astrocytes in the vascularized and non-vascularized retinal areas. Four random FOV per retina were examined (n=5). Error bars indicate s.d. Scale bars: 100 μm.

of *Gfap* mRNA in sorted PDGFRα$^+$ astrocytes from retinal tissues (Fig. 6B). Contrary to expectations, however, additional apelin in the WT retina did not alter blood vessel formation (Fig. 6A,C).

Next, we assessed whether apelin affected overgrowth by astrocytes in *Apln* KO mice. As in *APJ* KO mice, hyperproliferation of PDGFRα$^+$ PAX2$^+$ astrocytes was observed in *Apln* KO mice at P5 (Fig. 6D). Such astrocytes were weakly positive for GFAP (data not shown). Similar to the experiment shown in Fig. 6A, *Apln* KO mice at P3 were given intraocular injections of apelin and retinal gliogenesis was observed at P5. This demonstrated that apelin prevented the hyperproliferation of astrocytes that would otherwise result from the lack of apelin (Fig. 6D,E). Moreover, the capillary density in the migrating front of the vascular network was decreased in *Apln* KO mice injected intraocularly with apelin (Fig. 6D,F).

Because we failed to detect APJ expression in astrocytes, it is possible that ECs produce maturation factors for astrocytes when they are stimulated by apelin. We added supernatants from 24-hour apelin-stimulated cultures of cells of the bEnd3 EC line derived from mouse brain to primary cultures of retinal cells from WT mice at P1 (Fig. 7A). We did not detect a direct effect of apelin on the induction of GFAP expression by astrocytes, but these culture supernatants enhanced its expression in retinal cells. Candidate factors for inducing GFAP positivity in astrocytes are LIF and ciliary neurotrophic factor (CNTF), which are both members of the IL6 family (Kishimoto et al., 1995). We investigated the expression of IL6 family cytokines in PECAM1$^+$ ECs directly sorted from the retina of *APJ* KO mice or WT mice at P5. We could not detect IL6, oncostatin M, cardiotrophin 1 or IL11 in ECs from WT or *APJ* KO mice, and CNTF expression was similar in ECs from both sources. By contrast, LIF expression was markedly lower in *APJ* KO than in WT mice (Fig. 7B). Transcription of *LIF* was upregulated transiently upon stimulation of human umbilical vein ECs (HUVECs) with apelin (Fig. 7C). These data suggest that stimulation of ECs by apelin induces production of LIF in an APJ-dependent manner, which then influences astrocyte maturation.

Overgrowth of immature astrocytes resulting from a lack of APJ in ECs is abrogated by LIF injection

On the basis of the above results, we suggest that a lack of apelin/APJ system activity in ECs induces overgrowth of immature astrocytes followed by inhibition of their maturation,

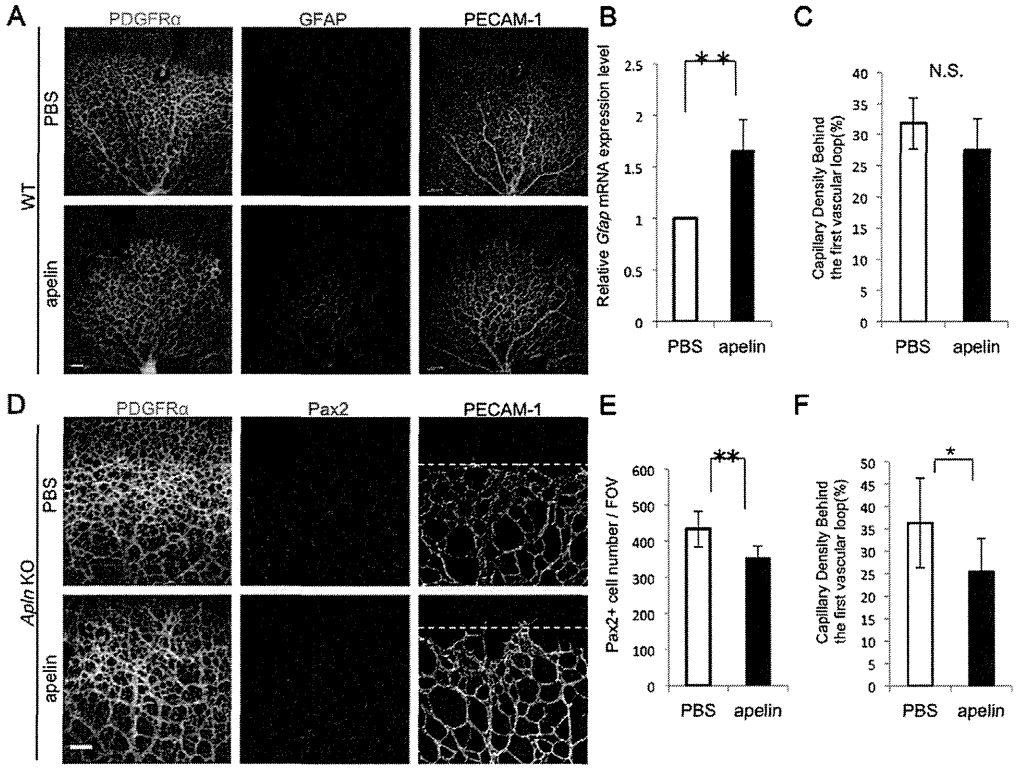

Fig. 6. Exogenous apelin-13 induces the expression of GFAP in retinal astrocytes. (**A-C**) Effect of apelin-13 in WT mouse retina. (A) Retinas were stained with antibodies against PDGFRα, GFAP and PECAM1 at P5, 48 hours after intraocular injection with PBS or apelin-13. (B) qPCR analysis of *Gfap* using mRNA from FACS-sorted PDGFRα$^+$ cells of P5 retina (**P<0.01). (C) Capillary density behind the first vascular loop after injection with apelin in WT mouse retina (n=6). N.S., not significant. (**D-F**) Rescue of aberrant overgrowth of astrocytes observed in *Apln* KO mice by intraocular injection of apelin-13. (D) Retinas were immunostained for PDGFRα, PAX2 and PECAM1 at P5, 48 hours after intraocular injection of PBS or apelin-13. (E) Quantitative evaluation of PAX2$^+$ astrocytes. Six random FOV in the retina were examined (n=6, **P<0.01). (F) Apelin reduces the capillary density from the vascular front in *Apln* KO mice (n=6, *P<0.05). The yellow dashed lines (D) demarcate the area (the first vascular loop) for which vascular density was calculated (C,F). Error bars indicate s.d. Scale bars: 100 μm.

resulting in aberrant EC network formation. Because LIF is upregulated upon stimulation of APJ by apelin in ECs, and because LIF is widely accepted as a maturation factor for astrocytes (Bonni et al., 1997; Mi et al., 2001), we injected LIF into *APJ* KO mice to assess whether maturation of astrocytes inhibits overgrowth of ECs as well as astrocytes. Intraocular injection of LIF into *APJ* KO mice at P3 resulted in a reduction of the number of PDGFRα$^+$ astrocytes and improved the formation of dense sheets of astrocytes (Fig. 7D). Moreover, weakly GFAP-positive astrocytes became strong GFAP expressors. Furthermore, staining with anti-PECAM1 antibody indicated that aberrant overgrowth of ECs was not induced. Quantitative evaluation of the number of astrocytes (confirmed by PAX2 staining) revealed that the hyperproliferation observed in the vascular area was reduced, but that LIF injection did not influence the number of astrocytes in the avascular area where no overgrowth had previously been observed (Fig. 7E). It is accepted that immature weakly GFAP-positive astrocytes induce proliferation of ECs but that this is gradually reduced as their level of GFAP expression increases (Kubota et al., 2008; West et al., 2005). This was suggested to be caused by the expression of VEGF in immature astrocytes. We assessed *Vegf* mRNA expression in retinal PDGFRα$^+$ astrocytes from *APJ* KO mice at P5. We found that LIF injection attenuated *Vegf* transcription (Fig. 7F), suggesting induction of astrocyte maturation.

DISCUSSION

Using a model of retinal angiogenesis, we have identified a possible mechanism by which maturation of astrocytes is induced as angiogenesis is finalized and newly developed blood vessels are consolidated. This entails apelin stimulation of APJ in ECs and subsequent LIF production, which induces maturation of weakly to strongly GFAP-positive astrocytes, which then enter quiescence. Because weakly GFAP-positive astrocytes act as proangiogenic accessory cells for ECs by producing VEGF and proliferate vigorously in response to PDGFA produced by ganglion cells, when LIF production is decreased due to the lack of apelin or APJ, the resulting aberrant overgrowth of immature astrocytes induces hyperproliferation of ECs. We propose that apelin/APJ activation in ECs is a trigger for finalization of blood vessel formation, indirectly mediated by the induction of astrocyte maturation.

We previously reported that although APJ is not expressed on ECs in the steady state after birth, in adulthood ischemia induces transient APJ expression in ECs mediated by stimulation with VEGF (Kidoya et al., 2008). In the retina, from the onset of retinal angiogenesis in newborn mice, network-forming ECs also transiently express APJ, which is downregulated after the establishment of the retinal endothelial network at P12 (Saint-Geniez et al., 2003). It has been reported using ISH that apelin is produced in tip cells, which might then induce proliferation of the stalk cells migrating behind them (del Toro et al., 2010). Apelin is secreted as peptides of 13 or 36 amino